hr 448 Pro のミオシリン変異を有する症例の報告[6)8)10)~12)14)]がみられる．そのうち Arg 46 Stop[12)]，Arg 158 Gln 変異[12)14)]を持つ症例は正常眼圧緑内障で，その他は開放隅角緑内障である．Arg 46 Stop は東洋人の多型とする報告[13)]もある．

今回の検索で，我々は Asp 208 Glu，Ile 360 Asn の新たな2種の変異をそれぞれ1家系ずつに見出した．Asp 208 Glu 変異は，当施設ではこれまでに100例中5例の対照例にみられていたため多型と判断していた[12)]．一方，本症例の他にも日本人および中国人で，同じ変異を有する緑内障症例が報告[13)]されており，緑内障の原因となる変異であるか議論されている．仮に今回の Asp 208 Glu 変異が緑内障を惹き起こすとすると，この家系において2例が正常眼圧緑内障を発病しており，1例は緑内障を発症していない．臨床型と変異型が完全に一致していないが，変異を持っている姉は35歳と若年であることから，今後，緑内障を発症する可能性もあり，最終的な診断のためには注意深い経過観察を要する．しかし，現時点ではこの Asp 208 Glu 変異は正常対照にもみられており，多型と考えるのが妥当であろう．

今回の Asp 208 Glu 変異とは別に，正常眼圧緑内障におけるミオシリン遺伝子変異例として，Gln 368 Stop[9)]，Arg 46 Stop[12)]，Arg 158 Gln 変異[12)14)]，Thr 293 Lys[16)]，Ile 499 Ser[17)]が報告されている．ミオシリンは，線維柱帯や Schlemm 管以外にも視神経乳頭部や網膜神経節細胞，虹彩毛様体，脳室などでの発現や局在が報告[7)18)~25)]されている．これまでにミオシリンの異常により緑内障が発症する機序として，線維柱帯の機能が障害され，房水流出抵抗が上昇し高眼圧となり緑内障が発症するという説が提唱されている．一方，ミオシリンは視神経乳頭部のアストロサイトの細胞内，細胞外に局在すると報告され，また，これらの細胞群は篩板組織における網膜神経節細胞軸索の構築を保ち，また神経栄養因子を分泌することによって網膜神経節細胞を栄養し，維持していると考えられている[18)19)]．以上から，ミオシリン異常によりこれら篩板部のアストロサイトの機能が低下する結果，視神経乳頭の脆弱性が増すことで正常眼圧緑内障を発症するのではないかと推察することもできる[18)19)]．Ile 360 Asn 変異はこれまで報告されていないが，この Ile 360 Asn 変異が正常対照にはなかったことから，原発開放隅角緑内障の原因と考えられる．この家系においては，遺伝子変異をもつ症例が緑内障，高眼圧症および正常所見を呈しており，同じ変異を持っていながら臨床表現型が異なっていた．しかし，発端者は50歳を過ぎてから緑内障と診断されているので，発端者の2人の娘は現在42歳および34歳であり，今後，加齢により緑内障を発症する危険が通常より高いと思われ，定期的に経過観察を行う予定である．

ミオシリンは当初，主として40歳未満発症の若年性開放隅角緑内障の原因遺伝子として報告[2)]された．しかし，今回同定された Ile 360 Asn 変異は，発端者が59歳発症と晩期発症型になっている．この家系のように晩期発症の開放隅角緑内障を来すミオシリン変異として，Gln 368 Stop 変異が報告[15)]されている．この変異は欧米で最も頻度が高いものであるが，ミオシリン変異としては特異的で40歳以降に発症する晩期発症型の開放隅角緑内障患者に多くみられる．しかし，その一方で発症年齢が40歳未満の例も存在し，また，60歳以上の健常者も存在する．さらに，家族性のみならず孤発の開放隅角緑内障患者[2)8)]や正常眼圧緑内障患者[9)]にも報告されている．したがって，緑内障は多因子疾患(または多遺伝子疾患)であり，ミオシリン変異を持っていても必ずしも発症せず，発症には加齢や環境要因などさらに何らかの因子が関与していることが考えられる．一方，若年発症の家系，例えば Gln 337 Arg 変異を持った家系[26)]では，変異を持った症例は全例5~21歳までに必ず発症しているので，ミオシリン変異の種類により，発症への関与は異なることが考えられる．

Asp 208 Glu 変異，Ile 360 Asn 変異および Gln 368 Stop 変異は，それ自体の変異では緑内障を発症するまでには至らないことがあり，その場合，他の何らかの因子が関与することで緑内障を発症する可能性がある．したがって，これらの変異は緑内障発症の危険因子としての意義が考えられる．今後はミオシリンの機能の解析と同時に，ミオシリン遺伝子変異を持つ緑内障症例とその家族の臨床情報を蓄積し，遺伝子変異の他にどのような危険因子が発病に影響しているかを解明して行くことが重要であると考えられた．

ご校閲を賜りました，慶應義塾大学医学部眼科学教室小口芳久教授に深謝いたします．

本論文の要旨は第11回日本緑内障学会で発表した．

本研究の一部は科学研究費補助金基盤研究C(課題番号12671723)奨励研究A(課題番号11771073)および日本学術振興会未来開拓事業による．

文　献

1) **Sheffield VC, Stone EM, Alward WL, Drack AV, Johnson AT, Streb LM,** et al：Genetic linkage of familial open angle glaucoma to chromosome 1q21-q31. Nat Genet 4：47—50, 1993.
2) **Stone EM, Fingert JH, Alward WLM, Nguyen TD, Polansky JR, Sunden SLF,** et al：Identification of a gene that causes primary open angle glaucoma. Science 275：668—670, 1997.
3) **Kubota R, Noda S, Wang Y, Minoshima S, Asakawa S, Kudoh J,** et al：A novel myosin-like protein (myocilin) expressed in the connecting cilium of the photoreceptor：Molecular cloning, tissue expression, and chromosomal mapping.

Genomics 41：360—369, 1997.

4) **Kubota R, Kudoh J, Mashima Y, Asakawa S, Minoshima S, Hejtmancik JF,** et al：Genomic organization of the human myocilin gene (MYOC) responsible for primary open angle glaucoma (GLC 1 A). Biochem Biophys Res Commun 242：396—400, 1998.

5) **Nguyen TD, Chen P, Huang WD, Chen H, Johnson D, Polansky JR**：Gene structure and properties of TIGR, an olfactomedin-related glycoprotein cloned from glucocorticoid-induced trabecular meshwork cells. J Biol Chem 273：6341—6350, 1998.

6) **Suzuki Y, Shirato S, Taniguchi F, Ohhara K, Nishimaki K, Ohta S**：Mutations in the TIGR gene in familial primary open-angle glaucoma in Japan. Am J Hum Genet 61：1202—1204, 1997.

7) **Allingham RR, Wiggs JL, Paz MADL, Vollrath D, Tallett DA, Broomer B,** et al：Gln 368 STOP myocilin mutation in families with late-onset primary open-angle glaucoma. Invest Ophthalmol Vis Sci 39：2288—2295, 1998.

8) **Fingert JH, Heon E, Liebmann JM, Yamamoto T, Craig JE, Rait J,** et al：Analysis of myocilin mutations in 1703 glaucoma patients from five different populations. Hum Mol Genet 8：899—905, 1999.

9) **Mardin CY, Velten I, Ozbey S, Rautenstrauss B, Michels-Rautenstrauss K**：A GLC 1 A gene Gln 368 Stop mutation in a patient with normal-tension open-angle glaucoma. J Glaucoma 8：154—156, 1999.

10) **Taniguchi F, Suzuki Y, Shirato S, Ohta S**：Clinical phenotype of a Japanese family with primary open angle glaucoma caused by a Pro 370 Leu mutation in the MYOC/TIGR gene. Jpn J Ophthalmol 43：80—84, 1999.

11) **Yokoyama A, Nao-i N, Date Y, Nakazato M, Chumann H, Chihara E,** et al：Detection of a new TIGR gene mutation in a Japanese family with primary open angle glaucoma. Jpn J Ophthalmol 43：85—88, 1999.

12) **Kubota R, Mashima Y, Ohtake Y, Tanino T, Kimura T, Hotta Y,** et al：Novel mutations in the myocilin gene in Japanese glaucoma patients. Hum Mutat 16：270, 2000.

13) **Lam DS, Leung YF, Chua JK, Baum L, Fan DS, Choy KW,** et al：Truncations in the TIGR gene in individuals with and without primary open-angle glaucoma. Invest Ophthalmol Vis Sci 41：1386—1391, 2000.

14) **Mabuchi F, Yamagata Z, Kashiwagi K, Ishijima K, Tang S, Iijima H,** et al：A sequence change (Arg 158 Gln) in the leucin zipper-like motif region of MYOC/TIGR protein. J Hum Genet 46：85—89, 2001.

15) **Angius A, Spinelli P, Ghilotti G, Casu G, Sole G, Loi A,** et al：Myocilin Gln 368 stop mutation and advanced age as risk factors for late-onset primary open-angle glaucoma. Arch Ophthalmol 118：674—679, 2000.

16) **Williams-Lyn D, Flanagan J, Buys Y, Trope GE, Fingert J, Stone EM,** et al：The genetic aspects of adult-onset glaucoma：A perspective from the Greater Toronto area. Can J Ophthalmol 35：12—17, 2000.

17) **Shimizu S, Lichter PR, Johnson AT, Zhou Z, Higashi M, Gottfredsdottir M,** et al：Age-dependent prevalence of mutations at the GLC1A locus in primary open-angle glaucoma. Am J Ophthalmol 130：165—177, 2000.

18) **Noda S, Mashima Y, Obazawa M, Kubota R, Oguchi Y, Kudoh J,** et al：Myocilin expression in the astrocytes of the optic nerve head. Biochem Biophys Res Commun 276：1129—1135, 2000.

19) **Clark AF, Kawase K, English-Wright S, Lane D, Steely HT, Yamamoto T,** et al：Expression of the glaucoma gene myocilin (MYOC) in the human optic nerve head. FASEB J 15：1251—1253, 2001.

20) **Polansky JR, Fauss DJ, Chen P, Chen H, Lütjen-Drecoll E, Johnson D,** et al：Cellular pharmacology and molecular biology of the trabecular meshwork inducible glucocorticoid response gene product. Ophthalmologica 211：126—139, 1997.

21) **Tamm ER, Russell P, Piatigorsky J**：Development and characterization of an immortal and differented murine trabecular meshwork cell line. Invest Ophthalmol Vis Sci 40：1392—1403, 1999.

22) **Takahashi H, Noda S, Imamura Y, Nagasawa A, Kubota R, Mashima Y,** et al：Mouse myocilin (Myoc) gene expression in ocular tissues. Biochem Biophys Res Commun 248：104—109, 1998.

23) **Swiderski RE, Ying L, Cassell MD, Alward WLM, Stone EM, Sheffield VC**：Expression pattern and *in situ* localization of the mouse homologue of the human MYOC (GLC1A) gene in adult brain. Mol Brain Res 68：64—72, 1999.

24) **Takahashi H, Noda S, Mashima Y, Kubota R, Ohtake Y, Tanino T,** et al：The myocilin (MYOC) gene expression in the human trabecular meshwork. Cur Eye Res 20：81—84, 2000.

25) **Wang X, Johnson DH**：mRNA *in situ* hybridization of TIGR/MYOC in human trabecular meshwork. Invest Ophthalmol Vis Sci 41：1724—1729, 2000.

26) **Stoilova D, Child A, Brice G, Crick RP, Fleck BW, Sarfarazi M**：Identification of a new 'TIGR' mutation in a family with juvenile-onset primary open angle glaucoma. Ophthalmic Genet 18：109—118, 1997.

シンポジウム

先天緑内障と遺伝子変異

真島 行彦

Gene mutations associated with congenital glaucoma

Yukihiko MASHIMA

I 緒　　言

緑内障は眼圧の上昇により視神経が圧迫され視神経萎縮を来たし，放置すると視野欠損を生じ，最後には失明に至る眼疾患である。原発性先天緑内障は通常1歳以内に発症し，角膜の混濁，流涙，しゅう明等の症状がみられる。先天緑内障は隅角の発育異常により，前房水の流出が障害されることにより眼圧上昇を来す。その結果，弾性ある新生児の眼球は拡大し，牛眼（buphthalmos）と呼ばれる状態になる（図1）。

先天緑内障の発症頻度は，欧州では5,000人から22,000人に1人，中近東では2,500人に1人，スロバキアのジプシーでは1,250人に1人と地域によりかなり異なる[1)~5)]。中近東やスロバキアのジプシーでは，先天緑内障が失明の上位を占める。日本においては，先天緑内障の発症頻度は不明である。先天緑内障の多くは家族歴がみられないが，約10%に常染色体劣性遺伝の家系が報告されている[6)]。また，男児の患者の方が多い[7)]。

成人も含めた緑内障は，失明原因としては第2位の疾患で，日本においては推定約200万人の患者が存在すると推測され，40歳以上の有病率は3-4%で，年齢と共に有病率は増加している。現在，原発性緑内障の原因となる疾患遺伝子が少なくとも8か所の染色体上にマッピングされている（表1）。原発性先天緑内障に関しては，1番染色体と2番染色体の2カ所に疾患遺伝子（それぞれ，GLC3BとGLC3A）が存在しており，GLC3Aは1997年に原発性先天緑内障の原因遺伝子，チトクロームP4501B1（遺伝子記号は*CYP1B1*）が明らかになった[8)]。この遺伝子の異常によって引き起こされる先天緑内障GLC3Aは，常染色体劣性遺伝病である。

慶應義塾大学医学部眼科学教室　〒160-8582　東京都新宿区信濃町35
Department of Ophthalmology, School of Medicine, University

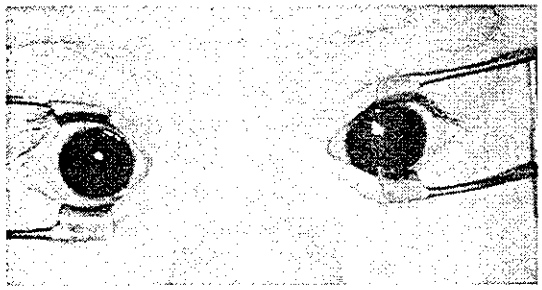

図1　先天緑内障患者にみられた牛眼（左眼）

表1　緑内障遺伝子と染色体マッピング

遺伝子座	染色体部位	遺伝子	緑内障の型	遺伝形式	診断年齢
GLC1A	1q23-25	MYOC	若年性開放隅角緑内障	常優	5-77歳
GLC1B	2cen-q13	不明	開放隅角緑内障	常優	>40
GLC1C	3q21-24	不明	開放隅角緑内障	常優	>40
GLC1D	8q23	不明	開放隅角緑内障	常優	
GLC1E	10p15-p14	OPTN	開放隅角緑内障	常優	23-65
GLC1F	7q35-q36	不明	開放隅角緑内障	常優	25-70
GLC3A	2p21	CYP1B1	先天緑内障	常劣	<3
GLC3B	1p36	不明	先天緑内障	常劣	<3

CLC1：開放隅角緑内障，GLC2：閉塞隅角緑内障，GLC3：先天緑内障（Human Genome Organization/Genome Database Nomenclature Comittee によるGLC分類）

今回，日本人先天緑内障患者におけるチトクロームP4501B1（*CYP1B1*）遺伝子解析を行い，変異を明らかにし[9)]，更に変異を持った患者の臨床像を検討した。

II 対象と方法

先天緑内障患者におけるチトクロームP4501B1

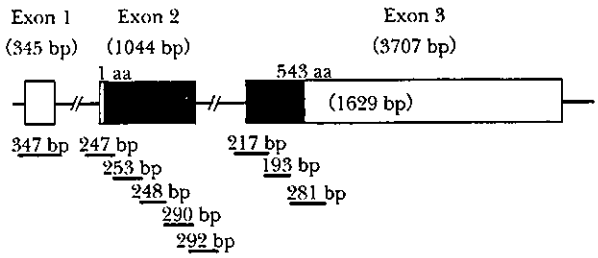

図2　チトクローム P4501B1（*CYP1B1*）遺伝子の解析

SSCP 解析を行うために，遺伝子を 9 ヵ所に分けて増幅した。

（*CYP1B1*）遺伝子解析は，生後 3 歳までに発症した原発性先天緑内障で，家系のそれぞれ異なる65症例を対象とした。内訳は，慶應義塾大学病院は28例（男児：女児＝18：10），東京大学病院は15例（5：10），旧国立小児病院（現在は国立生育医療センター）は15例（7：8），京都大学病院は 4 例（2：2），そして天理よろづ病院は 3 例（1：2）であった。これらの症例では，隅角発育異常の所見以外はなかった。

CYP1B1 遺伝子解析を行った先天緑内障患者のうち，発症からの臨床経過について調査しえた 32 症例について，性別，発症時期，前眼部・隅角所見などの臨床像を比較した。内訳は，変異を持った患者は11例で，持たない患者は21例であった。

CYP1B1 遺伝子の解析は，図 2 に示した様に，*CYP1B1* 遺伝子の翻訳領域を 9 カ所に分けて，PCR で増幅し，引き続き SSCP 法でスクリーニングした。SSCP 法で移動度に違いが見られれば，変異が疑われるので，塩基配列を決定した[9]。

Ⅲ 結　　果

1）チトクローム P4501B1（*CYP1B1*）遺伝子解析

図 3 に *CYP1B1* 遺伝子を解析した 1 家系を示す[10]。父親は片方の *CYP1B1* 遺伝子の364番目のアミノ酸を構成する 3 つの塩基の内，最初の G（グアニン）が A（アデニン）に変異したことにより，アミノ酸は Valine（GTG）から Methionine（ATG）に変異していた（Val364Met 変異）。その結果，チトクローム P4501B1 蛋白はの機能が障害されるものと考えられる。もう一方の *CYP1B1* 遺伝子は正常であった。すなわち，父親は保因者であった。

母親は片方の *CYP1B1* 遺伝子の324番目のアミノ酸（Isoleucine）を構成する 3 つの塩基，ATC において AT の後に更に AT の 2 つの塩基が新たに挿入されたため，アミノ酸への翻訳が正常とは異なり，325番目は異なる蛋白質が生成されることになる。そのために，チトクローム P4501B1 蛋白は機能が障害されるものと考えられる。もう一方の *CYP1B1* 遺伝子は正常であった。すなわち，母親も保因者であった。長女は両親の異常な *CYP1B1* 遺伝子を片方づつ受け継いだため，正常な *CYP1B1* 蛋白は生成されず，先天緑内障を発症したと考えられる。一方，次女は，母親から異常な *CYP1B1* 遺伝子を片方受け継ぎ，父親からは正常な *CYP1B1* 遺伝子を片方受け継いだため，発症せず，両親と同様に保因者となった。

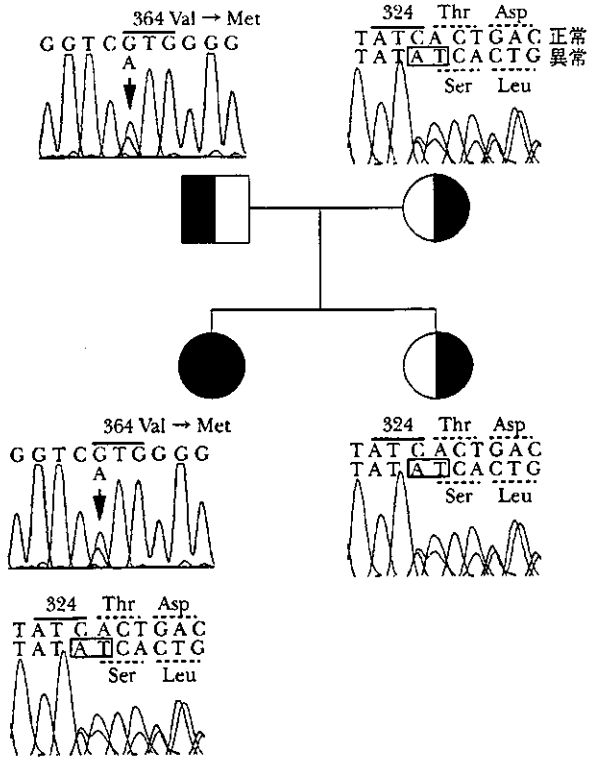

図3　チトクローム P4501B1（*CYP1B1*）遺伝子変異の 1 家系

先天緑内障は常染色体劣性遺伝疾患のため，患者は両親から遺伝子異常をそれぞれ受け継いでいる。父，母，次女は先天緑内障発症の保因者であることが分かる。

日本人先天緑内障患者では，65家系中13家系（20%）に日本人特有の11種類の新しい変異が確認された（表 2）。今回の日本人患者では血族結婚はみられず，13家系中ホモ変異（2 つの遺伝子変異が同じ場合で，両親が血族結婚の場合にみられることが多い）は 1 家系のみであり，他は複合ヘテロ変異（2 つの遺伝子変異が異なる場合）であった。11種類の変異の内，図 3 でみられた Val364Met 変異は 9 人中 6 人に確認された。ハプロタイプは調べていないが，創始者変異（ある 1 人の患者に突然出現した変異が後世に引き継がれてきた変異）の可能性はある。この変異をもつ患者は東日本在住が多かったので，東日本人に保因者が多く存在すると考えられる。一方，Arg444Gln 変異（Arginine が Glutamine に変異）は西日本に多くみられた変異であった。

表2　日本人先天緑内障患者にみられたCYP1B1遺伝子変異

家系数	塩基変化（塩基番号）	アミノ酸変化（コドン番号）
3	4776 insAT/G7927A	Frameshift/Val 364 Met
1	A4380T/A4380T	Asp 192 Val/Asp 192 Val
1	A4380T/G7927A	Asp 192 Val/Val 364 Met
1	G4793T, C4794T/G7927A	Ala 330 Phe/Val 364 Met
1	G7927A/G8168A	Val 364 Met/Arg 444 Gln
1	3964 del C/G8168A	Frameshift/Arg 444 Gln
1	C4645A/G8168A	Cys 280 stop/Arg 444 Gln
2	C3130T/G4763T	Unknown/Val 320 Leu
1	G4397A/Unidentified	Val 198 Ile/Unidentified
1	A8333G/Unidentified	Glu 499 Gly/Unidentified

13家系　（Mashima Y, et al. IOVS 42: 2211-2216, 2001）

表3　先天緑内障患者における性差と罹患眼

CYP1B1遺伝子	男児：女児	両眼：片眼
変異群	6例：5例	10例：1例
非変異群	19：2	17：4
Fishers'exact probability test	p＝0.03	p＝0.43

表4　先天緑内障患と診断された時期

CYP1B1遺伝子	診断された時期
変異群	平均1.8±3.2か月*（0-11か月）
非変異群	平均3.1±2.5か月*（0-8か月）

* P＝0.033 (Mann-Whitney U test)

2）チトクローム P4501B1（*CYP1B1*）変異患者の臨床像

*CYP1B1*変異を持った11症例（変異群）と持っていない21症例（非変異群）において，患者の性差は変異群ではほぼ1：1であったが，非変異群は男児が明らかに多かった。この性差に関して，有意差がみられた（表3）。両群とも両眼性が殆どであり，罹患眼に関して両群で有意差はなかった（表3）。診断時期に関して，変異群（1.8±3.2か月）の方が非変異群（3.1±2.5か月）よりも有意に早かった（表4）。その他，隅角や角膜所見に差はみられなかった。

N　考　　按

チトクローム P450181はチトクローム P450ファミリーに含まれる蛋白質のひとつで，培養細胞をダイオキシンで処理することによって誘発される遺伝子として知られている。肝臓に存在するチトクローム P450は薬物を酸化し，発癌物質等を解毒する。チトクローム P4501B1（*CYP1B1*）の cDNA は1994年に，遺伝子構造は1996年に報告された[11]。

最近，チトクローム P4501B1や他の薬物代謝酵素は発生，分化に関係する情報伝達系においてリガンドとして作用する酸化分子の安定性を制御している可能性が言われている[12]。すなわち，*CYP1B1*の変異は発生中の前眼部組織の構造や機能異常を来す可能性がある。そして，*CYP1B1*の変異が発生異常を起こした初めての疾患が先天緑内障 GLC3A である。

チトクローム P450ファミリーは様々な組織で発現しているが，*CYP1B1*は眼組織では隅角，毛様体，虹彩，無色素性の毛様体上皮に強い発現がみられるので，この部での発生に深く関わっている分子であることは間違いなく，今後，隅角の発生のメカニズムが分子レベルで解明されるきっかけになる蛋白である。眼外組織では心臓，脳，肺，肝臓，骨格筋，腎臓，膵臓とほとんどの組織に発現がみられるにも関わらず，その変異の影響は現在のところ隅角の発育異常だけに現れている。

*CYP1B1*変異に関して，サウジアラビア人では53家系中39家系の先天緑内障において共通のハプロタイプを持つ Gly61Glu 変異のホモ変異，3家系で Arg469Trp 変異のホモ変異をもっている[13)~15)]。スロバキアのジプシーでは，26家系の先天緑内障において共通のハプロタイプを持つ Glu387Lys 変異のホモ変異が報告されている[16)]。血族結婚が多いサウジアラビア，トルコ，スロバキアジプシーでは先天緑内障患者の85％は*CYP1B1*変異であり，これらの変異は創始者変異として各民族で蓄積されてきたことを示している。一方，日本人先天緑内障患者では，65家系中13家系（20％）に日本人特有の11種類の新しい変異が確認された。日本人患者では血族結婚はみられず，13家系中ホモ変異は1家系のみであり，他は複合ヘテロ変異であった。11種類の変異の内，Val364Met 変異は6人，Arg444Gln 変異は3人，コドン324の2塩基（AT）挿入は3人に確認され，頻度の高い変異であった。創始者変異の可能性はある。九州地方からも2種類の*CYP1B1*変異が報告されているが[17)18)]。その内の1つは Arg444Gln 変異[18)]である。日本人の先天緑内障患者の*CYP1B1*変異は日本人特有であり，また常染色体劣性遺伝病であることから，その種類は限られている可能性があり，今後 DNA チップによる患者および保因者の診断の可能性が考えられる。

*CYP1B1*変異を持った先天緑内障は，臨床所見に特徴的なものはなかったが，出生後早期に牛眼や角膜混濁の所見で発見される症例が多いのが特徴である。

V　要　　約

日本人先天緑内障患者におけるチトクローム P4501B1（*CYP1B1*）遺伝子解析を行い，変異を明らかにし，更に変異を持った患者の臨床像を検討した。対象は，生後3歳までに発症した家系のそれぞれ異なる原発

性先天緑内障65症例である。*CYP1B1* 遺伝子解析を行った先天緑内障患者のうち，発症からの臨床経過について調査しえた32症例（変異を持った患者は11例，持たない患者は21例）について，性別，発症時期，前眼部・隅角所見などの臨床像を比較した。

65家系中13家系（20%）に日本人特有の11種類の新しい変異が確認された。今回の日本人患者では血族結婚はみられず，13家系中ホモ変異は1家系のみであり，他は複合ヘテロ変異であった。*CYP1B1* 変異を持った11症例（変異群）と持っていない21症例（非変異群）において，患者の性差は変異群ではほぼ1：1であったが，非変異群は男児が明らかに多く，有意差がみられた。診断時期に関して，変異群（1.8±3.2か月）の方が非変異群（3.1±2.5か月）よりも有意に早かった。その他の臨床像に差はなかった。

CYP1B1 変異を持った先天緑内障は，臨床所見に特徴的なものはなかったが，出生後早期に牛眼や角膜混濁の所見で発見される症例が多いのが特徴である。

キーワード：先天緑内障，チトクローム P4501B1，牛眼，遺伝子変異

文　献

1) Travers JP: The presentation of congenital glaucoma. J Pediatr Ophthalmol Strabismus 16: 241—242, 1979.
2) Francois J: Congenital glaucoma and its inheritance. Ophthalmologica 181: 61—73, 1980.
3) Gencík A, Gencíkova A, Ferák V: Population genetical aspects of primary congenital glaucoma. I. Incidence, prevalence, gene frequency, and age of onset. Hum Genet 61: 193—197, 1982.
4) Jaffer MS: Care of the infantile glaucoma patient. In: Reineck RD, ed. Ophthalmology annual. New York: Raven Press; 15, 1988.
5) Wagner RS: Glaucoma in children. Pediatr Clin Nort Am 40: 855—867, 1993.
6) Gencík A: Epidemiology and genetics of primary congenital glaucoma in Slovakia. Description of a form of primary congenital glaucoma in gypsies with autosomal-recessive inheritance and complete penetrance. Dev Ophthalmol 16: 75—115, 1989.
7) Gencík A, Gencíkova A, Gerinec A: Genetic heterogeneity of congenital glaucoma. Clin Genet 17: 241—248, 1980.
8) Stoilov I, Akarsu AN, Sarfarazi M: Identification of three different truncating mutations in cytochrome P4501B1 (*CYP1B1*) as the principal cause of primary congenital glaucoma (Buphthalmos) in families linked to the GLC3A locus on chromosome 2p21. Hum Mol Genet 6: 641—647, 1997.
9) Mashima Y, Suzuki Y, Sergeev Y, et al: Novel cytochrome P4501B1 (*CYP1B1*) gene mutations in Japanese patients with primary congenital glaucoma. Invest Ophthalmol Vis Sci 42: 2211—2216, 2001.
10) Ohtake Y, Kubota R, Tanino T, Miyata H, Mashima Y: Novel compound heterozygous mutations in the cytochrome P450B1 gene (*CYP1B1*) in a Japanese patient with primary congenital glaucoma. Ophthalmic Genet 21: 191—193, 2000.
11) Tang YM, Wo YYP, et al: Isolation and characterization of the human cytochrome P450 *CYP1B1* gene. J Biol Chem 271: 28324—28330, 1996.
12) Nebert DW: Proposed role of drug-metabolizing enzyme: regulation of steady state levels of the ligands that effect growth, homeostasis, differentiation, and neuroendocrine functions. Mol Endocrinol 5: 1203—1214, 1991.
13) Stoilov I, Akarsu AN, Alozie I, et al: Sequence analysis and homology modeling suggest that primary congenital glaucoma on 2p21 results from mutations disrupting either the hinge region or the conserved core structures of cytochrome P4501B1. Am J Hum Genet 62: 573—584, 1998.
14) Bejjani BA, Lewis RA, Tomey KF, et al: Mutations in *CYP1B1*, the gene for cytochrome P4501B1, are the predominant cause of primary congenital glaucoma in Saudi Arabia. Am J Hum Genet 62: 325—333, 1998.
15) Bejjani BA, Stockton DW, Lewis RA, et al: Multiple *CYP1B1* mutations and incomplete penetrance in an inbred population segregating primary congenital glaucoma suggest frequent de novo events and a dominant modifier locus. Hum Mol Genet 9: 367—374, 2000.
16) Plásilová M, Stoilov I, Sarfarazi M, Kádasi L, Feráková E, Ferák V: Identification of a single ancestral *CYP1B1* mutation in Slovak Gypsies (Roms) affected with primary congenital glaucoma. J Med Genet 36: 290—294, 1999.
17) Kakiuchi T, Isashiki Y, Nakao K, Sonoda S, Kimura K, Ohba N: A novel truncating mutation of cytochrome P4501B1 (*CYP1B1*) gene in primary infantile glaucoma. Am J Ophthalmol 128: 370—372, 1999.
18) Kakiuchi-Matsumoto T, Iasashiki Y, Ohba N, et al: Cytochrome P4501B1 gene mutations in Japanese patients with primary congenital glaucoma. Am J Ophthalmol 131: 345—350, 2001.

Graefe's Arch Clin Exp Ophthalmol
(2003) 241:75–80

CLINICAL INVESTIGATION

DOI 10.1007/s00417-002-0598-0

Yukihiko Mashima
Itaru Kimura
Yusuke Yamamoto
Hisao Ohde
Yuichirou Ohtake
Tomihiko Tanino
Goji Tomita
Yoshihisa Oguchi

Optic disc excavation in the atrophic stage of Leber's hereditary optic neuropathy: comparison with normal tension glaucoma

Received: 25 June 2002
Revised: 15 October 2002
Accepted: 29 October 2002
Published online: 25 January 2003

Y. Mashima (✉) · I. Kimura · Y. Yamamoto
H. Ohde · Y. Ohtake · T. Tanino · Y. Oguchi
Department of Ophthalmology,
Keio University School of Medicine,
35 Shinanomachi, Shinjuku-ku,
160-8582 Tokyo, Japan
e-mail: mashima@sc.itc.keio.ac.jp
Tel.: +81-3-33531211 ext 62402
Fax: +81-3-33598302

G. Tomita
Department of Ophthalmology,
University of Tokyo Graduate School
of Medicine, Tokyo, Japan

Abstract *Background:* Abnormal optic disc excavations are reportedly seen in patients with Leber's hereditary optic neuropathy (LHON), a mitochondrial dysfunction disease. We examined the disc morphology in the eyes of patients with LHON at the atrophic stage and compared it to that in eyes with normal-tension glaucoma (NTG). *Methods:* We studied 15 LHON patients with the 11778 mutation, 15 patients with NTG, and 25 normal subjects. The optic disc morphology was analyzed by Heidelberg retinal tomography (HRT). Ten parameters of the optic disc obtained by HRT were evaluated, including the diagnostic classification of glaucoma. *Results:* Six of the nine morphological HRT parameters of the LHON patients, the exceptions being disc area, mean cup depth, and maximum cup depth, differed significantly from those of the normals. NTG patients had a significantly greater mean and maximum cup depth than LHON patients. The HRT glaucoma diagnostic software classified 22 (73%) of the 30 optic discs in LHON patients as glaucomatous. *Conclusion:* The optic discs at the atrophic stage of LHON eyes have glaucoma-like morphological changes. However, the cups were significantly deeper in NTG than LHON. The similarity in the optic disc findings in LHON and NTG suggests that alterations in mitochondrial function may be related to optic disc excavations.

Introduction

Leber's hereditary optic neuropathy (LHON) is a maternally-transmitted eye disease that mainly affects young adult men [15]. This disease usually causes severe and permanent loss of vision resulting in a visual acuity of less than 0.1. Visual field defects are present as central or cecocentral scotomas. In the acute stage of LHON, hyperemia of the disc and swelling of the peripapillary nerve fiber layer are often observed [15, 16]. These findings resolve over several months, leaving the optic disc pale on the temporal side in association with the disappearance of the papillomacular nerve fiber layer [16]. Within 1 year, most patients show pallor of the entire optic disc and experience profound and permanent loss of vision due to degeneration of retinal ganglion cells and optic nerve neurons.

More than 80% of LHON patients carry one of three mitochondrial DNA (mtDNA) mutations, at nucleotide position 3460, 11778, or 14484 [4, 13].

Abnormal cupping of the optic nerve head has been reported in the atrophic stage of LHON [12, 18, 19, 22, 24], but the cupping has not been quantitatively analyzed. The optic neuropathy of LHON has been mistaken for normal-tension glaucoma (NTG) [12], and has also been reported to develop in a family with NTG [24]. In addition, optic disc excavations in patients with autosomal dominant optic atrophy (ADOA; Kjer type), whose gene defect is related to mitochondrial integrity [6], have been misinterpreted as resulting from NTG [7].

Glaucomatous optic nerve damage is associated with the loss of the neuroretinal rim area, deepening of the optic cup, and enlargement of the parapapillary chorioretinal atrophy [11]. However, the appearance of an atro-

phic optic disc with excavation can result from different pathogenic mechanisms.

Confocal scanning laser ophthalmoscopy (HRT) using the Heidelberg Retina Tomograph (Heidelberg Engineering, Heidelberg, Germany) is a newly developed technique that can reconstruct and analyze the three-dimensional structure of the optic nerve head [20, 25]. HRT has been reported to be more accurate and reproducible than examiners' observations or computer-assisted analyses of stereoscopic optic disc photographs [5, 10, 20, 21].

In the present study, we retrospectively analyzed the three-dimensional images of the disc quantitatively in patients with LHON and NTG.

Patients and methods

LHON patients

Fifteen Japanese LHON outpatients who had a mtDNA mutation at nucleotide position 11778 and were under care for LHON at Keio University Hospital were examined by means of HRT between January 2000 and January 2001 (Table 1). All 15 patients, 13 men and 2 women, were at the atrophic stage of LHON. The age at the time of examination ranged from 16 to 46 years (mean ± SD; 27.8±8.7 years). The interval between the onset of the symptoms and the HRT examination ranged from 2 to 9 years. Refractive errors ranged from −5.50 to +0.50 diopters (D) (mean −2.11±1.47 D). Patients with atrophic optic discs had central scotomas or fenestrated central scotomas as demonstrated by either Goldmann perimetry or Humphrey perimetry using the 30-2 program. Their visual acuities ranged from 0.04 to 1.0. The mean deviations (MD) and corrected pattern standard deviations (CPSD) on Humphrey perimetry 30-2 in the eight patients (16 eyes) with visual acuities better than 0.2 were −18.4±8.3 dB (−7.2 to −33.0) and 7.4±2.3 dB (4.0–11.5), respectively.

All of the LHON patients showed pallor of the entire optic disc, and all had intraocular pressure (IOP) below 21 mmHg.

Normal-tension glaucoma patients

The NTG patients, enrolled during the same period as the LHON patients, included 10 men and 5 women; their age at the time of examination was 27–46 years (37.9± 5.3). The patients were diagnosed with NTG if the following conditions were fulfilled: the untreated peak IOP was equal to or less than 21 mmHg at all times, including the 24-h monitoring period; there was a normal open angle, typical glaucomatous disc cupping, and visual field changes; absence of ocular or systemic disorders that might have been responsible for the optic nerve damage. Patients with compression of the optic nerve confirmed by MRI or CT were excluded. The MD and CPSD on Humphrey perimetry 30-2 in the 15 patients (30 eyes) with NTG were −7.7±4.0 dB (−1.7 to −15.8) and 8.4±4.1 dB (1.6–15.4), respectively. Their corrected visual acuity was 1.2 or better, and their refractive errors ranged from −5.50 to +0.50 D (−2.53±1.60 D).

Normal subjects

Normal volunteers – 20 men and 5 women – were enrolled during the same period. Their corrected visual acuity was 1.2, and their ages were 23–41 years (27.7±4.2). Their refractive errors ranged from −5.50 to +0.50 D (−2.04±1.48 D). All subjects had an IOP below 21 mmHg. The MD and CPSD on Humphrey perimetry 30-2 in the 20 patients (40 eyes) were 0.98±2.5 dB and 1.3±0.9 dB, respectively.

Heidelberg retinal tomography

Heidelberg retinal tomography was performed in a standardized way by one examiner (I.K.). The optic disc in each eye was analyzed using the HRT version 2.01 software. A series of 32 confocal images in consecutive focal planes, each 256×256 pixels, were obtained with a confocal diode laser (670 nm). The computer then converted these images into a single topographic image. The depth of each topographic image ranged from 0.5 mm to 0.4 mm in 0.5-mm increments, depending on individual differences in the optic disc morphological characteristics. The field for each image was 10°×10°. Three images were obtained for each eye, and the mean of these three topographic image measurements was calculated for each pixel location. The mean topographic images, having less than 30 μm of average variability, were used.

The HRT glaucoma diagnostic software (the classification program) was applied automatically using the discriminant analysis formula developed by Mikelberg et al. [14] and Iester et al. [9]. If the solution of the equation was less than zero, the eye was considered glaucomatous; if the value was zero or greater, the eye was classified as nonglaucomatous.

Statistical analysis

The Mann–Whitney U-test was used to compare the data for age, refractive error, and nine HRT parameters between the normal group and the LHON group, or between the LHON group and the NTG group. P values <0.0055 (Bonferroni correction: 0.05/9 = 0.0055) were considered to show statistically significant differences.

Results

Fifty-five subjects were enrolled from January 2000 to January 2001, including 25 normal subjects (50 eyes), 15 patients with LHON at the atrophic stage (30 eyes), and 15 patients with NTG (30 eyes). No significant differences were found between the groups with regard to refraction (P >0.05), but patients with NTG were older than both the normal and the LHON subjects (P <0.01; Table 1).

Among the HRT parameters, nine values relating to disc morphology and the classification value for the 15 patients with LHON are listed in Table 1. Significant differences between the normal and LHON groups were found for six parameters: cup area, cup/disc area ratio, rim area, cup volume, rim volume, and cup shape. Neither the mean nor the maximum cup depth differed significantly between the normal and LHON groups.

On the other hand, significant differences were found between the LHON and NTG groups for the mean cup depth and maximum cup depth. The mean and maximum cup depth were significantly greater in the NTG than in the LHON patients (P = 0.001). The optic disc in a patient with LHON (case 1) who showed the largest values

Table 1 Heidelberg Retina Tomograph parameters in patients with Leber's hereditary optic atrophy (*LHON*; *NTG* normal-tension glaucoma)

Case	Age (years)	Gender	R/L	Visual acuity	Disk area (mm^2)	Cup (mm^2)	Cup/disk area ratio	Rim area (mm^2)	Cup volume (mm^3)	Rim volume (mm^3)	Mean cup depth (mm)	Maximum cup depth (mm)	Cup shape measure	Classification
1	16	M	R	1.0	2.569	1.587	0.618	0.982	0.456	0.152	0.338	0.712	−0.074	−2.77
			L	0.8	2.758	1.760	0.638	0.998	0.607	0.130	0.368	0.816	−0.074	−2.94
2	31	M	R	0.3	2.372	1.240	0.523	1.132	0.167	0.078	0.134	0.390	−0.189	−0.85
			L	0.06	2.493	1.549	0.622	0.943	0.256	0.120	0.209	0.454	−0.045	−2.90
3	20	M	R	1.0	2.296	0.768	0.335	1.528	0.110	0.513	0.239	0.595	−0.134	0.80
			L	1.0	2.148	0.932	0.434	1.216	0.163	0.359	0.246	0.506	−0.051	−1.77
4	21	M	R	0.3	2.614	1.170	0.448	1.444	0.369	0.197	0.252	0.663	−0.173	−0.85
			L	0.2	2.158	0.876	0.406	1.282	0.248	0.140	0.216	0.631	−0.223	−0.72
5	29	F	R	0.03	1.488	0.674	0.453	0.814	0.079	0.081	0.136	0.338	−0.112	−2.20
			L	0.02	1.894	0.814	0.430	1.079	0.111	0.174	0.191	0.391	−0.033	−2.37
6	23	M	R	1.0	1.651	0.514	0.311	1.137	0.037	0.251	0.160	0.408	−0.160	−0.98
			L	0.09	1.955	0.931	0.476	1.024	0.129	0.208	0.242	0.483	−0.007	−3.27
7	34	M	R	0.04	2.139	0.862	0.403	1.277	0.206	0.270	0.252	0.595	−0.115	−1.40
			L	0.06	2.197	1.014	0.461	1.183	0.227	0.208	0.246	0.575	−0.128	−1.39
8	26	M	R	0.03	2.968	2.115	0.712	0.853	0.553	0.091	0.281	0.541	0.023	−4.63
			L	0.04	3.047	1.683	0.552	1.364	0.308	0.161	0.208	0.455	−0.052	−2.55
9	28	M	R	0.02	2.150	0.750	0.349	1.401	0.151	0.322	0.230	0.621	−0.176	−0.04
			L	0.02	1.529	0.544	0.356	0.985	0.103	0.247	0.237	0.660	−0.181	−1.17
10	20	M	R	0.9	1.931	0.657	0.340	1.274	0.070	0.414	0.265	0.599	−0.084	−1.41
			L	0.7	2.535	1.462	0.577	1.073	0.318	0.189	0.281	0.618	−0.061	−2.80
11	46	M	R	0.02	2.664	1.470	0.552	1.194	0.264	0.107	0.185	0.476	−0.139	−1.11
			L	0.01	2.568	1.670	0.650	0.898	0.303	0.079	0.181	0.482	−0.141	−2.21
12	30	F	R	0.9	1.810	0.739	0.408	1.071	0.059	0.255	0.193	0.376	−0.006	−2.85
			L	0.8	2.157	0.689	0.319	1.468	0.091	0.435	0.211	0.448	−0.078	0.14
13	43	M	R	0.02	2.102	0.290	0.138	1.812	0.028	0.399	0.113	0.344	−0.217	2.44
			L	0.02	1.952	0.447	0.229	1.505	0.062	0.339	0.124	0.415	−0.279	1.99
14	32	M	R	0.5	2.333	0.489	0.209	1.845	0.026	0.510	0.119	0.332	−0.151	1.53
			L	0.06	2.426	0.740	0.205	1.686	0.077	0.385	0.135	0.343	−0.131	0.85
15	18	M	R	1.0	3.054	0.809	0.265	2.244	0.116	0.595	0.188	0.483	−0.158	2.58
			L	1.0	3.012	0.696	0.231	2.316	0.063	0.727	0.169	0.419	−0.121	3.59
LHON	27.8 ± 8.7				2.30 ± 0.43	1.0 ± 0.46	0.42 ± 0.15	1.30 ± 0.38	0.19 ± 0.15	0.27 ± 0.17	0.21 ± 0.06	0.53 ± 0.11	− 0.12 ± 0.07	
NTG	37.9 ± 5.3				2.21 ± 0.53	1.09 ± 0.44	0.49 ± 0.15	1.11 ± 0.42	0.28 ± 0.19	0.23 ± 0.10	0.29 ± 0.09	0.63 ± 0.15	− 0.09 ± 0.09	
P value*	0.001				0.209	0.359	0.115	0.046	0.066	0.579	0.001	0.001	0.231	
LHON	27.8 ± 8.7				2.30 ± 0.43	1.0 ± 0.46	0.42 ± 0.15	1.30 ± 0.38	0.19 ± 0.15	0.27 ± 0.17	0.21 ± 0.06	0.53 ± 0.11	− 0.12 ± 0.07	
Normal	27.7 ± 4.2				2.05 ± 0.41	0.53 ± 0.37	0.24 ± 0.13	1.58 ± 0.29	0.10 ± 0.14	0.42 ± 0.15	0.19 ± 0.06	0.54 ± 0.12	− 0.28 ± 0.39	
P value*	0.77				0.015	0.001	0.001	0.001	0.005	0.001	0.33	0.075	0.001	

*Mann–Whitney U-test

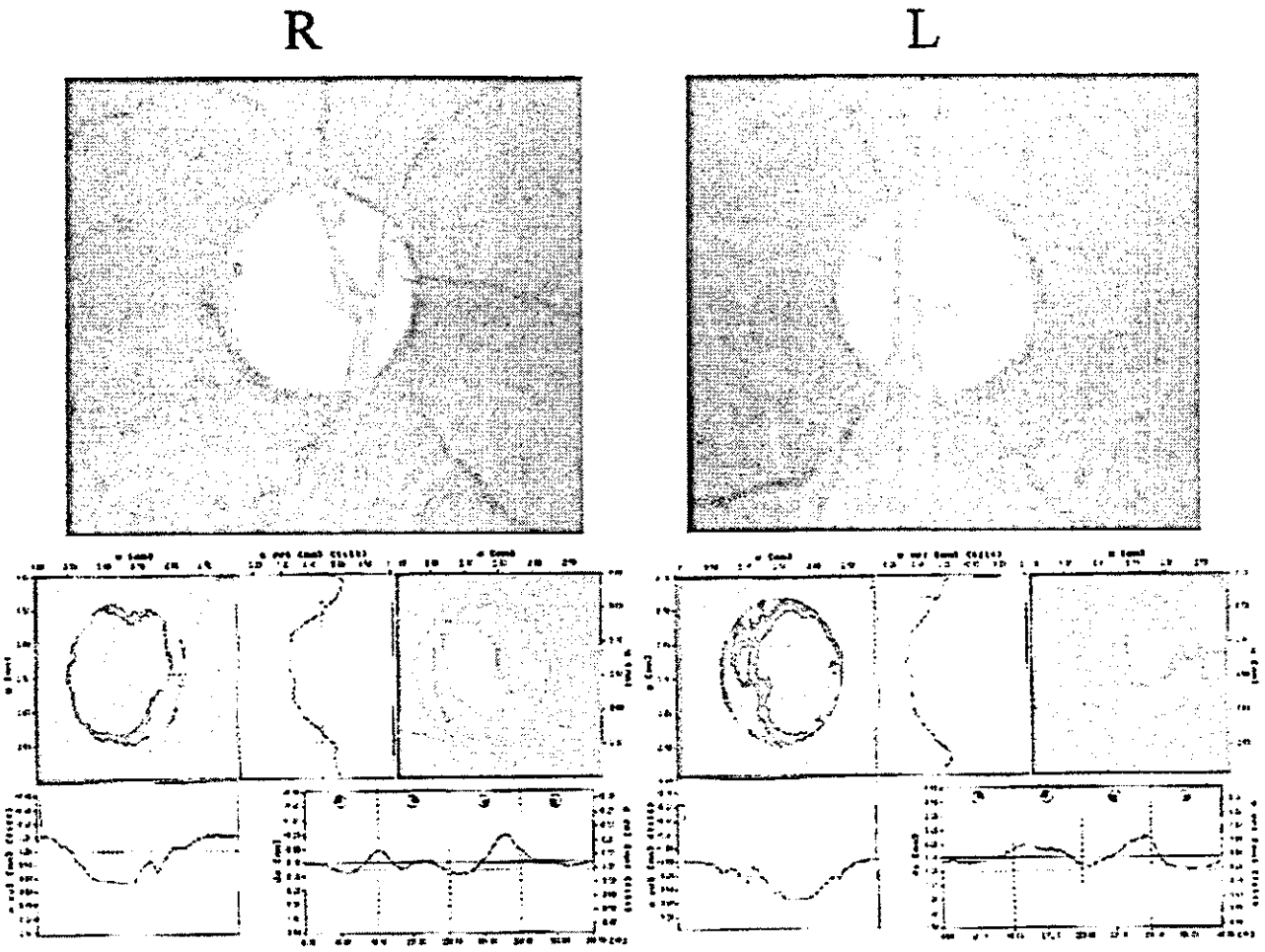

Fig. 1 Optic disc appearance in a patient with LHON who had the largest mean cup depth and largest maximum cup depth (case 1). Maps obtained by HRT analysis are shown below the fundus photographs. In both eyes, the cupping of the optic disc is displayed in *red* in the topographic map (*middle left*). Vertical (*middle center*) and horizontal (*bottom left*) cross-sectional profiles of the cupping are also displayed. Deep cupping is prominent particularly in the superior portion of the optic disc cup in both eyes. The contour line of the optic disc margin (*bottom right*) represents height variation of the nerve fiber layer surface at the disc margin

for mean and maximum cup depth is shown in Fig. 1. The optic disc of a LHON patient (case 8) who showed the largest classification value (–4.63 in the right eye and –2.55 in the left eye) is shown in Fig. 2.

The classification program misidentified 22 (73%) of 30 eyes of LHON patients as glaucomatous, while finding 26 (87%) of 30 eyes of the NTG patients to be glaucomatous. Four (8%) of 50 eyes of normal subjects were misidentified as glaucomatous.

Discussion

Abnormal cupping has been reported to be present at the atrophic stage of LHON. Trobe et al. [22] described disc cupping in 20% of 16 eyes with LHON (5% considered glaucomatous and 15% considered nonglaucomatous), while Radius and Maumenee [19] reported mildly increased cupping in 27 patients with congenital optic atrophy, six of whom had LHON. The similarity in the morphology of the optic disc in patients with LHON and glaucoma can lead to misdiagnosis, as Lauer et al. [12] reported for a patient with LHON who was referred for surgical treatment of progressive NTG. More recently, Ortiz et al. [18] reported significantly larger optic cups and optic atrophy in LHON family members with the 11778 mutation. Weiner et al. [24] reported the development of progressive optic disc cupping after the onset of LHON in a 54-year-old woman with the 11778 mutation. She had a family history of NTG.

We obtained quantitative values of the optic disc variables by means of HRT in eyes with atrophic LHON and NTG as well as in eyes of normal subjects. The optic

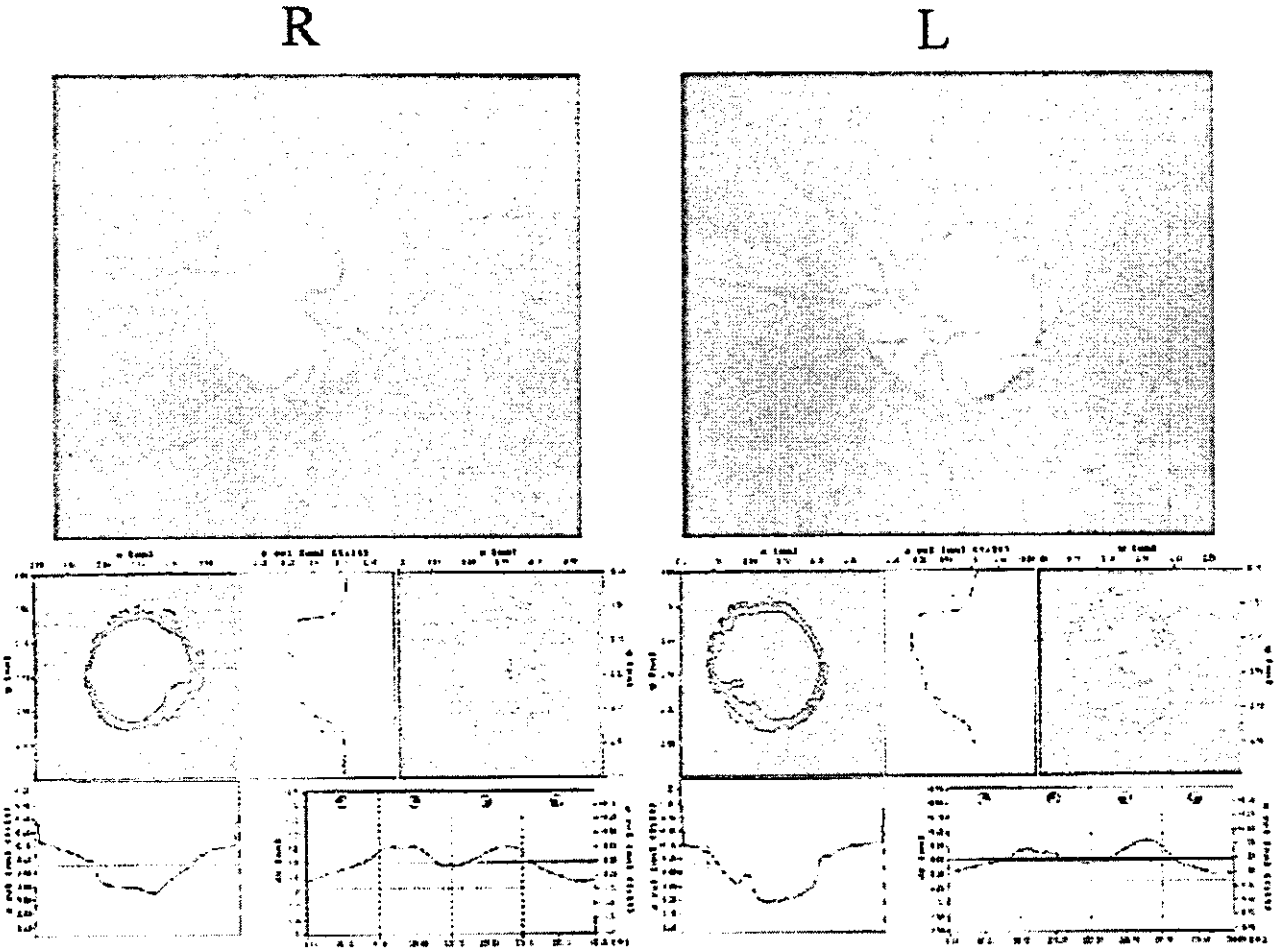

Fig. 2 Optic disc appearance in a patient with LHON who had the highest classification program values, suggesting a glaucomatous cup (case 8: –4.63 in the right eye and –2.55 in the left eye). Maps obtained by HRT analysis are shown below the fundus photographs. In both eyes, the cupping of the optic disc is displayed in *red* in the topographic map (*middle left*). The cupping extends almost to the optic disc margin, and the neuroretinal rim on the temporal half of the disc is almost absent in both eyes. Vertical (*middle center*) and horizontal (*bottom left*) cross-sectional profiles of the cupping are also displayed. The contour line of the optic disc margin (*bottom right*) represents height variation of the nerve fiber layer surface at the disc margin

disc at the atrophic stage of LHON exhibited cupping similar to that in glaucoma. Of the nine HRT parameters, seven were not significantly different between patients with LHON and NTG. The classification program of HRT identified a high percentage (73%) of eyes of LHON patients as having glaucoma-like cupping. Eyes with LHON and NTG, however, were significantly different for two parameters: mean cup depth (P=0.001), and maximum cup depth (P=0.001). Thus, the cup depth parameters may be valuable in differentiating optic nerve cupping caused by glaucoma from that in LHON patients. However, some patients with LHON, as seen in Figs. 1 and 2, showed prominent glaucoma-like cupping that was difficult to differentiate from glaucoma by HRT measurements. In such LHON patients, the main feature distinguishing the LHON discs from the discs of NTG was the pallor of the remaining neuroretinal rim. All of the LHON patients showed pallor of the entire optic disc, while the glaucoma patients showed localized or diffuse loss of the neuroretinal rim.

Loss of unmyelinated axons from the prelaminar optic nerve can result in increased disc excavation in LHON patients [18]. In addition to the marked loss of the nerve fiber layer, other factors may underlie the abnormal excavation in patients with LHON. Glaucomatous cupping has been histologically shown to result from the loss of both axons and astroglia in the optic disc [1, 8]. Progressive cupping of the optic disc results from compression, stretching, and remodeling of the connective tissue of the lamina cribrosa. Astrocytes are likely to be responsible for the remodeling of the optic nerve head in glaucomatous eyes [23]. In LHON, the astrocytes might be direct-

ly damaged as a consequence of the 11778 mutation. Optic disc astrocytes in LHON may become atrophic, permitting remodeling of tissues into a scar. Although NTG patients were tested for the three LHON mutations of mtDNA nucleotide positions 3460, 11778, and 14484 to test the hypothesis that NTG had a pathogenesis similar to LHON, no mutations and no defects in respiratory chain activity in skeletal muscle samples were detected [3, 17]. As this series of NTG patients were not examined for the LHON-associated mtDNA mutations, we cannot exclude this hypothesis.

Large optic cups have been reported in patients with ADOA (Kjer type) [7, 22]. The gene (*OPA1*) responsible for ADOA encodes a dynamin-related protein localized to mitochondria [6]. Thus, the abnormal disc excavation in these two diseases suggests that alterations in mitochondrial function may be responsible for the disc excavation. Recently, polymorphisms in the *OPA1* gene have been reported to be associated with NTG [2]. However, whether gene defects affecting mitochondrial function might contribute to the development of excavation in patients with NTG is not known.

References

1. Anderson DR, Cynader MS (1997) Glaucomatous optic nerve cupping as an optic neuropathy. Clin Neurosci 4:274–278
2. Aung T, Ocaka L, Ebenezer ND et al. (2002) A major marker for normal tension glaucoma: association with polymorphisms in the OPA1 gene. Hum Genet 110:52–56
3. Brierley EJ, Griffiths PG, Weber K, et al (1996) Normal respiratory chain function in patients with low-tension glaucoma. Arch Ophthalmol 114:142–146
4. Brown MD, Wallace DC (1994) Spectrum of mitochondrial DNA mutations in Leber's hereditary optic neuropathy. Clin Neurosci 2:138–145
5. Chauhan BC, LeBlanc RP, McCormick TA, et al (1994) Test–retest variability of topographic measurements with confocal scanning laser tomography in patients with glaucoma and control subjects. Am J Ophthalmol 118:9–15
6. Delettre C, Lenaers G, Griffoin JM, et al (2000) Nuclear gene OPA1, encoding a mitochondrial dynamin-related protein, is mutated in dominant optic atrophy. Nat Genet 26:207–210
7. Fournier AV, Damji KF, Epstein DL, et al (2001) Disc excavation in dominant optic atrophy. Differentiation from normal tension glaucoma. Ophthalmology 108:1595–1602
8. Hernandez MR, Pena JD (1997) The optic nerve head in glaucomatous optic neuropathy. Arch Ophthalmol 115:389–395
9. Iester M, Mikelberg FS, Drance SM (1997) The effect of optic disc size on diagnostic precision with the Heidelberg retina tomograph. Ophthalmology 104:545–548
10. Janknecht P, Funk J (1994) Optic nerve head analyser and Heidelberg retina tomograph: accuracy and reproducibility of topographic measurements in a model eye and in volunteers. Br J Ophthalmol 78:760–768
11. Jonas JB, Budde WM, Panda-Jonas S (1999) Ophthalmoscopic evaluation of the optic nerve head. Surv Ophthalmol 43:293–320
12. Lauer SA, Ackerman J, Sunness J, et al (1985) Leber's optic atrophy with myopia masquerading as glaucoma: case report. Ann Ophthalmol 17:146–148
13. Mackey DA, Oostra RJ, Rosenberg T, et al (1996) Primary pathogenic mtDNA mutations in multigeneration pedigrees with Leber hereditary optic neuropathy. Am J Hum Genet 59:481–485
14. Mikelberg FS, Parfitt CM, Swindale NV, et al (1995) Ability of the Heidelberg retina tomograph to detect early glaucomatous visual field loss. J Glaucoma 4:242–247
15. Newman NJ (1998) Hereditary optic neuropathies. In: Miller NR, Newman NJ (eds) Walsh and Hoyt's clinical neuro-ophthalmology, Vol I, 5th edn. Williams and Wilkins, Baltimore, pp 741-773
16. Nikoskelainen E, Hoyt WF, Nummelin K (1983) Ophthalmoscopic findings in Leber's hereditary optic neuropathy. II. The fundus findings in the affected family members. Arch Ophthalmol 101:1059–1068
17. Opial D, Boehnke M, Tadesse S, et al (2001) Leber's hereditary optic neuropathy mitochondrial DNA mutations in normal-tension glaucoma. Graefes Arch Clin Exp Ophthalmol 239:437–440
18. Ortiz RG, Newman NJ, Manoukian SV, et al (1992) Optic disk cupping and electrocardiographic abnormalities in an American pedigree with Leber's hereditary optic neuropathy. Am J Ophthalmol 113:561–566
19. Radius RL, Maumenee AE (1978) Optic atrophy and glaucomatous cupping. Am J Ophthalmol 85:145–153
20. Rohrschneider K, Burk RO, Kruse FE, et al (1994) Reproducibility of the optic nerve head topography with a new laser tomographic scanning device. Ophthalmology 101:1044–1049
21. Shields MB, Tiedeman JS, Miller KN, et al (1989) Accuracy of topographic measurements with the Optic Nerve Head Analyzer. Am J Ophthalmol 107:273–279
22. Trobe JD, Glaser JS, Cassady JC (1980) Optic atrophy. Differential diagnosis by fundus observation alone. Arch Ophthalmol 98:1040–1045
23. Varela HJ, Hernandez MR (1997) Astrocyte responses in human optic nerve head with primary open-angle glaucoma. J Glaucoma 5:303–313
24. Weiner NC, Newman NJ, Lessell S, et al (1993) Atypical Leber's hereditary optic neuropathy with molecular confirmation. Arch Neurol 50:470–473
25. Weinreb RN, Lusky M, Bartsch DU, et al (1993) Effect of repetitive imaging on topographic measurements of the optic nerve head. Arch Ophthalmol 111:636–638

CLINICAL SCIENCE

Phenotype of cytochrome P4501B1 gene (*CYP1B1*) mutations in Japanese patients with primary congenital glaucoma

Y Ohtake, T Tanino, Y Suzuki, H Miyata, M Taomoto, N Azuma, H Tanihara, M Araie, Y Mashima

Br J Ophthalmol 2003;**87**:302–304

See end of article for authors' affiliations

Correspondence to: Yuichiro Ohtake, MD, Department of Ophthalmology, Keio University School of Medicine, 35 Shinanomachi, Shinjuku-ku, Tokyo 160–8582, Japan; ohtake@dmb.med.keio.ac.jp

Accepted for publication 30 August 2002

Aim: To investigate the phenotypes associated with cytochrome P4501B1 gene (*CYP1B1*) mutations in Japanese patients with primary congenital glaucoma (PCG).

Methods: 66 Japanese patients with PCG were screened for sequence mutations in the *CYP1B1* gene using single strand conformation polymorphism analysis followed by automated DNA sequencing. 11 cases had a *CYP1B1* mutation in both alleles (the mutation group) and 21 cases did not have a *CYP1B1* mutation (the "no mutation" group). The clinical features, such as age of onset, sex, intraocular pressure, and Descemet's membrane rupture, of the two groups were compared.

Results: The clinical symptoms and signs did not differ for the two groups. The mean age at onset was 1.7 months in the mutation group and 3.1 months in the no mutation group, and the male:female ratio was 6:5 in the mutation group and 19:2 in the no mutation group. Both of these differences were statistically significant.

Conclusions: In clinically diagnosed cases of PCG, a subgroup shows a *CYP1B1* gene mutation. Age at onset was earlier in PCG patients with *CYP1B1* mutations than in patients without mutations. Women were more prevalent among patients with mutations than those without mutations.

Primary congenital glaucoma (PCG; gene symbol, GLC3) is a group of disorders characterised by an improper development of the eye's aqueous outflow system.[1–4] PCG is detected clinically in neonates and infants by the increased intraocular pressure (IOP). Because the coating of the infantile eye is elastic, it stretches in response to the elevated IOP, resulting in an enlarged globe (buphthalmos).[3 4]

PCG is inherited as an autosomal recessive trait, and the incidence varies geographically; one in 5000 to one in 22 000 newborns in Western countries, one in 2500 in the Middle East, and one in 1250 in the gipsy population of Slovakia, among whom PCG is the major cause of blindness.[1 5–8] In Japan, the incidence of PCG has not been determined, but most cases are sporadic.[9]

Two PCG mutation loci have been identified—the GLC3A locus which maps to chromosome 2p21[10] and the GLC3B locus which maps to chromosome 1p36.[11] Recently, several mutations in the cytochrome P4501B1 gene, *CYP1B1*, have been reported in families with PCG linked to the GLC3A locus.[9 12–18] *CYP1B1* gene mutations were detected in over 85% of families with PCG in Saudi Arabia, Turkey, and Slovakia.[12–15] Recently, we screened the *CYP1B1* gene in 65 unrelated Japanese probands with PCG and identified 11 novel mutations in 13 probands (20%).[9]

We present a more detailed investigation of the relation between the phenotype of Japanese patients with PCG and the genotype of *CYP1B1* mutation.

SUBJECTS AND METHODS

Blood samples were collected from 66 patients (65 families) with PCG at the following hospitals: 28 at Keio University Hospital, 16 at Tokyo University Hospital, 15 at the National Children's Hospital, three at Kyoto University Hospital, and four at Tenri Yorozu Hospital. Patients with elevated IOP associated with other ocular or systemic anomalies were excluded. None of these Japanese probands was the offspring of a consanguineous marriage. All cases except for one pair of twin girls (cases 8 and 9) in the group with mutations appeared to be sporadic with no family history of glaucoma. Informed consent was obtained from the parents of each child as well as their own participation in the study. This investigation was performed according to the guidelines of the Declaration of Helsinki.

Genomic DNA was prepared from leucocytes by proteinase K-phenol-chloroform extraction. We first screened the *CYP1B1* gene (GenBank accession number U56438) by polymerase chain reaction (PCR) amplification followed by single strand conformation polymorphism (SSCP) analysis as described previously.[9]

Clinical features at initial presentation

The clinical features at the onset of PCG were ascertained in 32 cases by examining the clinical records at each hospital. Of the 32 PCG patients, 11 had a *CYP1B1* mutation in both alleles (the "mutation group"), while 21 had no mutation (the "no mutation" group). We compared the mutation group with the no mutation group in terms of sex, age at diagnosis of PCG, and appearance of anterior segment (for example, corneal opacity, Descemet's membrane rupture, and gonioscopic appearance). For analysis, the onset of PCG was defined as the time of the initial diagnosis.

RESULTS

All cases in the mutation and no mutation group had typical symptoms and signs of PCG such as tearing, photophobia, and corneal enlargement. The clinical and genetic information of the 11 patients with *CYP1B1* mutations is summarised in Table 1.

The male:female ratio was 6:5 in the mutation group and 19:2 in the no mutation group (Table 2). This difference was significant (Fisher's exact probability test: $p < 0.05$). In comparison, previous reports have estimated that male cases account for approximately 65% of PCG cases overall.[3 4] Patients with bilateral PCG included 10 (91%) of 11 cases with the

Table 1 Clinical and genotypic information in 11 Japanese patients with primary congenital glaucoma (mutation group)

Case	Sex	Age at onset	Affected eye	Corneal opacity	Ruptures in Descemet's membrane	Mutations in CYP1B1 gene	
1	F	2 weeks	B	R+/L+	R+/L+	4776 ins AT (Frameshift)	G 7927 A (Val 364 Met)
2	M	2 months	B	+/−	−/−	4776 ins AT (Frameshift)	G 7927 A (Val 364 Met)
3	M	1 month	B	+/+	−/−	C 4645 A (Cys 280 stop)	G 8168 A (Arg 444 Gln)
4	F	at birth	B	+/+	−/−	3964del C (Frameshift)	G 8168 A (Arg 444 Gln)
5	M	at birth	B	+/+	+/+	G 7927 A (Val 364 Met)	G 8168 A (Arg 444 Gln)
6	M	at birth	B	+/+	−/+	A 4380 T (Asp 192 Val)*	
7	F	at birth	B	+/+	+/−	4776 ins AT (Frameshift)	G 7927 A (Val 364 Met)
8	F	1 week	B	+/+	−/−	G4793T,C4794T (Ala 330 Phe)	G 7927 A (Val 364 Met)
9	F	1 week	B	+/+	−/+	G4793T,C4794T (Ala 330 Phe)	G 7927 A (Val 364 Met)
10	M	2 months	B	+/+	−/−	A 4380 T (Asp 192 Val)	G 7927 A (Val 364 Met)
11	M	11 months	L	−/+	−/+	C3130T (Unknown)†	G 4763 T (Val 320 Leu)

B = bilateral, R = right, L = left.
*Homozygous; †Probable mutation in the noncoding region of exon 1.

Table 2 Clinical signs in primary congenital glaucoma patients with or without *CYP1B1* mutations

	Male: female*	Bilateral: unilateral	Mean age at onset**
Mutation group	6:5	10:1	1.7 months (0–11)
No mutation group	19:2	17:4	3.1 months (0–8)

*Fisher's exact probability test; $p<0.05$.
**Mann-Whitney test; $p<0.05$.

CYP1B1 mutation, and 17 (81%) of 21 cases without the *CYP1B1* mutation (Table 2). This finding without mutation is in agreement with previous reports that the disease is bilateral in approximately 75% of cases.[3]

The PCG was always diagnosed at birth or within the first year of life. A significant difference was evident in mean age at onset (3.1 months in the no mutation group and 1.7 months in the mutation group, Table 2; Mann-Whitney test, $p<0.05$). More specifically, 10 cases in the mutation group (all except for one case with a C3130T mutation, case 11) were diagnosed as PCG within 2 months of birth.

Most cases had corneal opacity and ruptures in Descemet's membrane (Table 3). No differences in the clinical findings were found between the two groups. Gonioscopy showed that most cases had a high insertion of the iris (Table 3), but we could not strictly classify anterior angle appearance because of corneal opacities and the retrospective, multicentre design of the study. One case had an atypical, unilateral uveal ectropion on the pupillary margin (case 4).

We present the clinical features of two atypical cases (4 and 11), and a unique pair of identical twins (8 and 9) with the *CYP1B1* mutation.

Case 4

A newborn Japanese girl was referred to Kyoto University Hospital for evaluation of corneal opacities of both eyes. No contributory family history or consanguinity was present. The IOPs, measured during sleep were 25 mm Hg for right eye and 30 mm Hg for left eye. The horizontal corneal diameter was 10.5 mm for right eye and 11.0 mm for left eye. Diffuse corneal opacities were present in both eyes, but no rupture in Descemet's membrane was present. Corneal opacities prevented a clear examination of the anterior chamber angles by gonioscopy. But the pupils were round and both irises were slightly atrophic in colour. The crystalline lenses and the vitreous cavity were normal. The optic discs showed slight glaucomatous cupping, with cup to disc ratios of 0.3 for right eye and 0.5 for left eye.

Genetic analysis showed that she was a compound heterozygote with both 3964delC and Arg444Gln mutations.

The patient underwent trabeculotomies once in the right eye and twice in the left eye, and the IOPs were controlled at 9–18 mm Hg (right eye) and 12 to 22 mm Hg (left eye) for 5 years.

When she was 3 years old, a uveal ectropion was observed at the pupillary margin of the left eye. Corrected visual acuity on a recent examination was 0.5 for right eye and 0.02 for left eye.

Case 11

An 11 month old Japanese boy, who was a compound heterozygote with both the C3130T and Val320Leu mutations, was referred to the National Children's Hospital for evaluation of a corneal enlargement and opacity in left eye. No contributory family history or consanguinity was present. The IOPs were 13 mm Hg for right eye and 50 mm Hg for left eye. The patient was diagnosed with PCG and subsequently examined under anaesthesia. The horizontal corneal diameter was 11.5 mm in the right eye and 12.5 mm in the left eye. Ruptures in Descemet's membrane were observed in the left eye. Gonioscopy revealed that the anterior chamber angles were widely open with anterior iris insertion, most markedly in the left eye. The crystalline lenses and the vitreous were normal. The left optic disc had glaucomatous cupping with the cup to disc ratio of 0.8; the right disc appeared normal.

Trabeculotomy was performed on the left eye, and the IOP was controlled between 8 and 18 mm Hg for 6 years. The corrected visual acuity on a recent examination was limited to 0.05 because of amblyopia probably caused by corneal opacity.

Cases 8 and 9

These identical twin girls, who were compound heterozygotes with both Ala330Phe and Val364Met, were referred to the

Table 3 Anterior segment appearance in primary congenital glaucoma with or without *CYP1B1* mutations

	Corneal opacity	Ruptures in Descemet's membrane	High insertion of iris
Mutation group	20/21 eyes (95.2%)	8/21 eyes (38.1%)	17/21 eyes (80.9%)
No mutation group	35/38 eyes (92.1%)	16/38 eyes (42.1%)	32/38 eyes (84.2%)

Tokyo University Hospital as newborns for evaluation of corneal opacities in both eyes. Both cases were affected bilaterally with PCG, and the increased IOP was detected within 1 week of age. The IOPs were elevated in both eyes, and clinical features such as corneal opacities and gonioscopic appearance were very similar in the twins. Goniotomies were performed on both eyes of the twin. But the IOPs could not be controlled on the left eye of case 9, and finally Scheie's sclerostomy was performed after two goniotomies. The final corrected visual acuity was 0.8 for right eye and 0.7 for left eye in case 8, and 0.1 for right eye and no perception of light for left eye in case 9.

DISCUSSION

The rarity of PCG and its differing frequency among ethnic groups impedes analysis of the phenotype and genotype of *CYP1B1* mutations. We are not aware of a previous report discussing the phenotypes of patients with and without *CYP1B1* mutations. In our Japanese patients with PCG, 11 cases had a *CYP1B1* mutation in both alleles and 23 cases did not have a mutation in the *CYP1B1* gene.

CYP1B1 gene mutations have been identified in over 85% of PCG affected families in Saudi Arabia, Turkey, and Slovakia.[13–15] However, a 27% prevalence of *CYP1B1* mutation has been reported in cases with sporadic occurrence.[16] This finding is similar to that of our earlier study, in which a 20% mutation rate was found in the Japanese PCG patients.[9]

In our present investigation, comparisons between the *CYP1B1* mutation group and the no mutation group revealed significant differences in sex preponderance and age at glaucoma onset. Interestingly, 10 cases in the mutation group, all except case 11, had bilateral involvement, and the first signs of disease appeared within 2 months of birth. In addition, compared to the no mutation group, the proportion of female patients was significantly higher in the mutation group. These features such as sex preponderance and bilateral incidence were very similar to PCG patients with the *CYP1B1* mutations in Saudi Arabia, Turkey, and India.[13 14 17] It is not clear why the sex ratios are so different between the two groups, as opposed to the fact that males account for approximately 65% of PCG cases overall.[3 4] We suggest that there may be another subtype of PCG with a higher preponderance in males, and these patients may have mutations not linked to the *CYP1B1* but to an unknown genetic locus.

Maldevelopment of the anterior segment may involve the trabecular meshwork alone or the trabecular meshwork in combination with the iris and/or cornea. Although PCG is a specific term referring to eyes that have an isolated maldevelopment of the trabecular meshwork without other ocular developmental anomalies or diseases that can raise the IOP, the terminology for glaucomas affecting infants has been inconsistent and sometimes confusing.[3 4] In our case 4, a unique uveal ectropion was observed in one of the affected eyes. Thus, a new classification of glaucomas affecting infants might be based on the presence or absence of a *CYP1B1* gene mutation.

A male patient (case 11), who was a compound heterozygote with both C3130T and Val320Leu alterations, was diagnosed relatively late in life as having unilateral glaucoma. In this case, the initial signs of glaucoma were identified when the patient was 11 months old, a relatively late detection time, and the anterior chamber developmental anomalies were found in both eyes (although pressure was elevated in only one eye). Thus, this C3130T mutation may partially inhibit normal cytochrome P4501B1 expression, leading to incomplete anterior chamber development and be manifested as a relatively mild case of PCG.

We had also a pair of identical twin girls with the *CYP1B1* gene mutation (cases 8 and 9). There was a concordance in the phenotypic features due to the same genetic factor, but the final visual acuity was different for the two cases. Although we should consider both the surgical efficacy and the influence of amblyopia, some environmental factors as well as genetic factors might modulate the severity of the disease.

In conclusion, among Japanese patients clinically diagnosed with PCG, we found a subtype with *CYP1B1* gene mutations. Clarification of how the *CYP1B1* gene is related to anterior chamber development may lead to better understanding of the mechanism of PCG occurrence and fundamental changes in the treatment of PCG.

Authors' affiliations
Y Ohtake, T Tanino, H Miyata, Y Mashima, Department of Ophthalmology, Keio University School of Medicine, Japan
Y Suzuki, M Araie, Department of Ophthalmology, University of Tokyo Graduate School of Medicine, Japan
M Taomoto, Department of Ophthalmology, Tenri Yorozu Hospital, Nara, Japan
N Azuma, Department of Ophthalmology, National Children's Hospital, Tokyo, Japan
H Tanihara, Department of Ophthalmology, Kumamoto University School of Medicine Japan

REFERENCES

1 **François J.** Congenital glaucoma and its inheritance. *Ophthalmologica* 1980;**181**:61–73.
2 **Hoskins HD,** Shaffer RN, Hetherington J. Anatomical classification of the developmental glaucomas. *Arch Ophthalmol* 1984;**102**:1331–6.
3 **Dickens CJ,** Hoskins HD. Congenital glaucoma. In: Ritch R, Shields MB, Krupin T, eds. *The glaucomas.* 2nd ed. St Louis, MO: Mosby, 1996:727–49.
4 **Stamper RL,** Lieberman MF, Drake MV. Developmental and childhood glaucoma. In: *Becker-Shaffer's diagnosis and therapy of the glaucomas.* 7th ed. St Louis, MO: Mosby, 1999:361–411.
5 **Travers JP.** The presentation of congenital glaucoma. *J Pediatr Ophthalmol Strabismus* 1979;**16**:241–2.
6 **Gencik A,** Gencikova A, Ferak V. Population genetical aspects of primary congenital glaucoma. I: incidence, prevalence, gene frequency, and age of onset. *Hum Genet* 1982;**61**:193–7.
7 **Jaffer MS.** Care of the infantile glaucoma patient. In: Reineck, RD ed. *Ophthalmology annual 15.* New York: Raven Press, 1988.
8 **Wagner RS.** Glaucoma in children. *Pediatr Clin North Am* 1993;**40**:855–67.
9 **Mashima Y,** Suzuki Y, Sergeev Y, *et al.* Novel cytochrome P4501B1 (CYP1B1) gene mutations in Japanese patients with primary congenital glaucoma. *Invest Ophthalmol Vis Sci* 2001;**42**:2211–6.
10 **Sarfarazi M,** Akarsu AN, Hossain A, *et al.* Assignment of a locus (GLC3A) for primary congenital glaucoma (buphthalmos) to 2p21 and evidence for genetic heterogeneity. *Genomics* 1995;**30**:171–7.
11 **Akarsu AN,** Turacli ME, Aktan SG, *et al.* A second locus (GLC3B) for primary congenital glaucoma (buphthalmos) maps to the 1p36 region. *Hum Mol Genet* 1996;**5**:1199–203.
12 **Stoilov I,** Akarsu AN, Sarfarazi M. Identification of three different truncating mutations in cytochrome P4501B1 (CYP1B1) as the principal cause of primary congenital glaucoma (buphthalmos) in families linked to the GLC3A locus on chromosome 2p21. *Hum Mol Genet* 1997;**6**:641–7.
13 **Bejjani BA,** Lewis RA, Tomey KF, *et al.* Mutations in CYP1B1, the gene for cytochrome P4501B1, are the predominant cause of primary congenital glaucoma in Saudi Arabia. *Am J Hum Genet* 1998;**62**:325–33.
14 **Stoilov I,** Akarsu AN, Alozie I, *et al.* Sequence analysis and homology modeling suggest that primary congenital glaucoma on 2p21 results from mutations disrupting either the hinge region or the conserved core structures of cytochrome P4501B1. *Am J Hum Genet* 1998;**62**:573–84.
15 **Plasilova M,** Stoilov I, Sarfarazi M, *et al.* Identification of a single ancestral CYP1B1 mutation in Slovak gypsies (Roms) affected with primary congenital glaucoma. *J Med Genet* 1999;**36**:290–4.
16 **Sarfarazi M,** Stoilov I. Molecular genetics of primary congenital glaucoma. *Eye* 2000;**14**:422–8.
17 **Panicker SG,** Reddy AB, Mandal AK, *et al.* Identification of novel mutations causing familial primary congenital glaucoma in Indian pedigrees. *Invest Ophthalmol Vis Sci* 2002;**43**:1358–66.
18 **Stoilov IR,** Costa VP, Vasconcellos JP, *et al.* Molecular genetics of primary congenital glaucoma in Brazil. *Invest Ophthalmol Vis Sci* 2002;**43**:1820–7.

Available online at www.sciencedirect.com
SCIENCE DIRECT®
Clinical Biochemistry 37 (2004) 268–276
CLINICAL BIOCHEMISTRY

Rapid quantification of the heteroplasmy of mutant mitochondrial DNAs in Leber's hereditary optic neuropathy using the Invader technology

Yukihiko Mashima,[a,*] Makoto Nagano,[b] Tomoyo Funayama,[a] Qiang Zhang,[a] Tohru Egashira,[b] Jun Kudho,[c] Nobuyoshi Shimizu,[c] and Yoshihisa Oguchi[a]

[a] *Department of Ophthalmology, Keio University School of Medicine, Shinjuku, Tokyo 160-8582, Japan*
[b] *Research Department, R&D Center, BML, 1361-1 Matoba, Kawagoe, Saitama 350-1101, Japan*
[c] *Department of Molecular Biology, Keio University School of Medicine, Shinjuku, Tokyo 160-8582, Japan*

Received 26 August 2003; received in revised form 20 November 2003; accepted 20 November 2003

Abstract

Purpose: To quantify the degree of heteroplasmy of a mitochondrial DNA (mtDNA) mutation in Leber's hereditary optic neuropathy (LHON) a biplex Invader® assay was applied.

Methods: To determine the optimum condition for the Invader® assay, mtDNAs were assayed in various amounts of total DNA in 1–4-h incubations at 63 °C. To evaluate the suitability of the Invader® assay to detect the three mutations, G3460A, G11778A, and T14484C, 10 ng of DNAs from 224 patients with bilateral optic atrophy was assayed. To quantify mtDNA heteroplasmy, a standard curve of known mixture ratios of mutation against calculation by the Invader® assay was constructed. Seventy-two of the 224 patients had one of the three mutations, which corresponded with the mutation detected earlier by polymerase chain reaction restriction fragment length polymorphism (PCR-RFLP) analysis. The percentages of mutant mtDNAs were calculated by the Invader® assay in five heteroplasmic families, including 30 individuals with the G11778A mutation. The results were compared with those calculated earlier by labeled polymerase chain reaction followed by single-strand conformation polymorphism (PCR-SSCP) analysis.

Results: In 1–8 ng of DNA, the fluorescence intensity increased near linearly during a 4-h assay. With more than 16 ng of DNA, the intensities were saturated even at the 2-h assay. A linear relationship was observed between the results obtained from separate mixtures and from the Invader® assay analysis. Because two fluorescent intensities are not always the same, one of the two intensities was modified to adjust to that of the other. Complete concordance was observed between PCR-RFLP analysis and Invader® assay genotyping for the 224 patients. Results of percentage of heteroplasmy in five LHON families obtained by the Invader® assay were consistent with those by the PCR-SSCP analysis.

Conclusions: Invader® assay is a simple, rapid, and reliable method of genotyping mtDNA mutations as well as quantifying heteroplasmy simultaneously under optimum conditions.

Keywords: G11778A mutation; G3460A mutation; T14484CA mutation; Heteroplasmy; Invader technology; Leber's hereditary optic neuropathy; Mitochondrial DNA

Introduction

Leber's hereditary optic neuropathy (LHON) is a maternally inherited disease and is associated with acute or subacute bilateral loss of central vision that mainly affects young men [1]. Visual field defects are observed as central or cecocentral absolute scotomas. Within 1 year of onset, most patients show total pallor of the optic disc and suffer a profound and permanent loss of vision due to the degeneration of retinal ganglion cells and optic nerve neurons.

More than 90% of LHON patients carry one of three mutations at nucleotide positions (np) 3460, 11778, and 14484 of the mitochondrial DNA (mtDNA) [2–4]. In families carrying inherited disorders with mtDNA point mutations, some maternal relatives are found to have a

* Corresponding author. Department of Ophthalmology, Keio University School of Medicine, 35 Shinanomachi, Shinjuku, Tokyo 160-8582, Japan. Fax: +81-3-3359-8302.
E-mail address: mashima@sc.itc.keio.ac.jp (Y. Mashima).

0009-9120/$ - see front matter © 2003 The Canadian Society of Clinical Chemists. All rights reserved.
doi:10.1016/j.clinbiochem.2003.11.011

mixture of mutant and wild-type mtDNAs, a condition known as heteroplasmy. Some heteroplasmic lineages segregate during cell division toward the homoplasmic state, the presence of only one genotype of the wild-type or mutant mtDNA, while others still remain heteroplasmic [5]. Heteroplasmic individuals are more likely to remain asymptomatic than homoplasmic ones [6–9]. In LHON patients with the 11778 mutation, heteroplasmy can be detected in about 14% of the families [10,11]. A correlation between the extent of heteroplasmy in the circulating leukocytes and the risk of developing optic atrophy or the severity of the disease has been reported in some pedigrees of LHON [10–17]. Identifying such at-risk individuals offers an opportunity to provide better genetic counseling.

To quantify the degree of heteroplasmic mtDNA mutation at np11778, we have developed a technique that uses polymerase chain reaction followed by single-strand conformation polymorphism (PCR-SSCP) analysis using ^{32}P-labeled PCR primers [11]. Other methods to evaluate heteroplasmy have been reported for experimental use [12,13,15,18–20]. Although the PCR restriction fragment length polymorphism (PCR-RFLP) followed by densitometry analysis is a simple, rapid, and most commonly used method to clinically determine the level of heteroplasmy, partial digestion due to heteroduplex formation during PCR often causes incomplete cleavage at the restriction site [21].

We have developed a technique to quantify the degree of heteroplasmy of mtDNA mutations using a new biplex invader technology, an Invader® assay (Third Wave Technologies, Inc, Madison, WI). This method was recently developed to determine genotyping single nucleotide polymorphism (SNP) and has been used for high-throughput genotyping [22–26]. Invader® assay, a non-PCR-based assay, consists of the hybridization of two oligonucleotides (a discriminatory primary probe and an Invader® oligonucleotide) to the target DNA forming an overlapping structure, that is, the substrate for a structure-specific 5′nuclease termed Cleavase (Fig. 1). The 5′end of the primary probe includes a 5′-flap sequence that does not hybridize to the target DNA. The Cleavase® enzyme recognizes this overlapping structure and cleaves off the unpaired 5′flap of the primary probe, resulting it as a target-specific product. In a secondary invasive reaction, each cleaved 5′flap in turn can serve as an Invader® oligonucleotide on a fluorescence resonance energy transfer (FRET) cassette to create another overlapping structure that is recognized and cleaved by the Cleavase® enzyme. The generated fluorescence signals are detected at an arbitrary time end point with a conventional fluorescence plate reader [27]. The biplex format uses two different discriminatory primary probes, each with a unique 5′ flap, and two different FRET cassettes, each with a spectrally distinct fluorophore, which allows for the detection of alleles of a given SNP in a single reaction. This method is highly sensitive and specific for detection of alleles of a given SNP in a single reaction. Our results indicate that this non-PCR method can also be used to quantify the degree of mtDNA heteroplasmy in a simple, rapid, and reliable way in LHON.

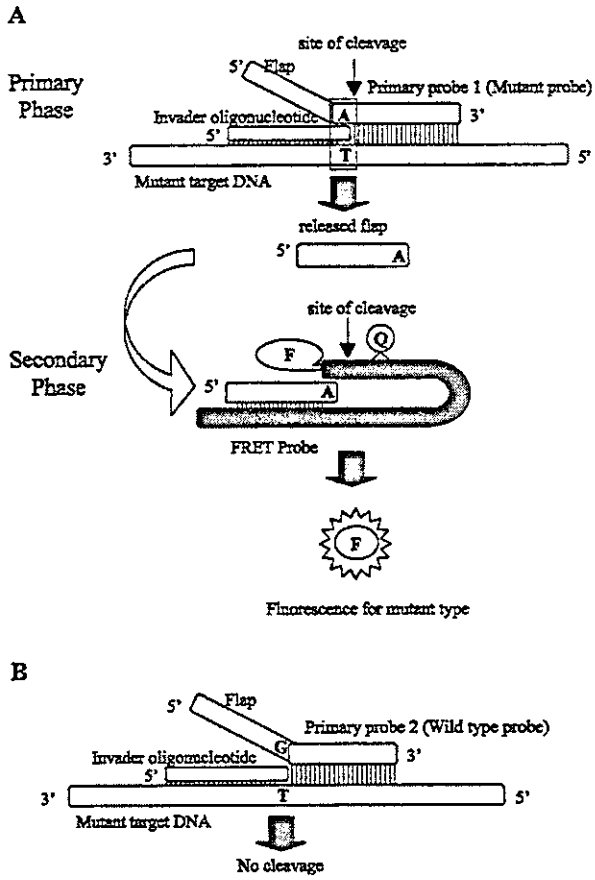

Fig. 1. Schematic representation of single-base discrimination and detection with the Invader® assay. (A) During the primary phase, an Invader® oligo and a primary probe are annealed to target DNA, overlapping at the SNP position (rectangular box). The arrow indicates the site of cleavage by the Cleavase enzyme. The released 5′flap anneals to the FRET cassette during the second phase and indicates a second cleavage reaction that releases the fluorescent dye. The signal is only released when the invasion structure is formed on the target DNA. (B) If the primary probe does not match the nucleotide at the SNP position, Cleavase does not act and cleavage of the primary probe does not occur. F, fluorescein; Q, quencer.

Methods

Patients

We tested 224 unrelated patients with bilateral optic atrophy or optic neuropathy, and 70 of their maternal relatives for five primary point mutations in mtDNA at np3460, np9804, np11778, np13730, and np14484. Their genotype had been demonstrated by PCR-RFLP analysis between 1991 and 1998 at Keio University Hospital [4,11,28]. The human research followed the tenets of the Declaration of Helsinki. Informed consent was obtained

after the nature and possible consequences of the study were explained. Seventy-two (32%) of the 224 patients had one of the three mtDNA mutations; 63 patients (88%) had the G11778A mutation, 6 patients (8%) had the T14484C mutation, and 3 patients (4%) had the G3460A mutation [28].

To evaluate the suitability of the Invader® assay for detecting the three mutations, the 224 patients were reexamined by this new method. We further selected five heteroplasmic families including 30 individuals with the G11778A mutation [11] and quantified the percentage of mutant mtDNA by using the Invader® assay. Results were compared with those determined by labeled PCR-SSCP analysis earlier [11].

Detection of mtDNA mutation by Invader® assay

The primary probes (wild and mutant probes) and the Invader® oligonucleotides (Invader® probe) used to detect the three mtDNA mutations (G3460A, G11778A, and T14484C) by the Invader® assay are shown in Table 1. Invader® assay FRET-detection 96-well plates (Third Wave Technologies, Inc) contain the generic components of an Invader® assay (Cleavase® enzyme VIII, FRET probes, MOPS buffer, and polyethylene glycol) dried in each of the individual wells.

The probe–Invader®–$MgCl_2$ mixture was prepared by combining 3 μl of primary probe–Invader® mix and 5 μl of 22.5 mM $MgCl_2$ per reaction. The primary probe–Invader® mixture contained 3.5 μmol/l wild primary probe, 3.5 μmol/l mutant primary probe, 0.35 μmol/l Invader® oligonucleotide, and 10 mmol/l MOPS. Eight microliters of the primary probe–Invader®–$MgCl_2$ mixture was added to each well of a 96-well plate. Seven microliters of 5 pmol/l synthetic target oligonucleotides, 10 μg/ml yeast tRNA (no target control, NTC), and total DNA (10 ng) samples consisting a mixture of genomic and mitochondrial DNA were added and were denatured by incubation at 95 °C for 10 min. After 15 μl of mineral oil (Sigma, St. Louis, MO) was overlaid on all reaction wells, the plate was incubated isothermally at 63 °C for 1–4 h in a PTC-100 thermal cycler (MJ Research, Waltham, MA) and then kept at 4 °C until

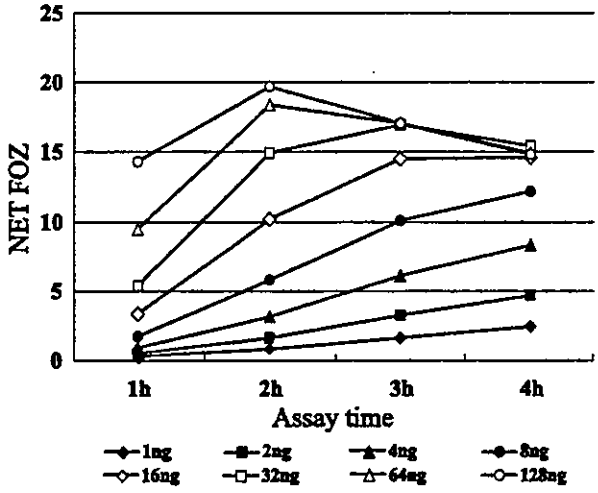

Fig. 2. Relationship between NET FOZ values and assay time for eight different amounts of DNA for the Invader® assay.

fluorescence measurements. The fluorescence intensities were measured on a CytoFlour 4000 fluorescence plate reader (Applied Biosystems, Foster City, CA) with excitation at 485 nm/20 nm (wavelength/bandwidth) and emission at 530 nm/25 nm for FAM dye; excitation at 560 nm/20 nm and emission at 620 nm/40 nm for Redmond RED (RED) dye.

Each sample was tested in duplicate in the same plate and two fluorescence measurements were performed in each plate. Thus, four measurements were obtained for each sample and were averaged. The signal/background, or Fold Over Zero (FOZ), is used to confirm the validity of each assay of the samples [29]. FOZ values were determined as follows: Probe 1, FOZ = FAM raw counts from sample / FAM raw counts from no target control (NTC); Probe 2, FOZ = RED raw counts from sample/RED raw counts from NTC. The two FOZ values for each sample are used to calculate the allelic ratio which was defined as follows: (Probe 1 FOZ-1)/(Probe 2 FOZ-1) = NET FAM FOZ/NET RED FOZ. These values were calculated by the program provided by Third Wave Technologies. Allelic ratio can

Table 1
The oligonucleotide sequence of wild type, mutant, and Invader probes with Invader assay to detect mutations of mtDNA

Position Mutation	Nucleotide	Target	Probe	Sequence	Tm	Dye
NADH dehydrogenase subunit Ala52Thr	G3460A	Anti-sense	Wild	**ACGGACGCGGAG**gccataaaactcttcacca	63.2	RED
			Mutant	**CGCGCCGAGG**accataaaactcttcaccaaa	63.3	FAM
			Invader	ccctacgggctactacaacccttcgctgact	77.7	
NADH dehydrogenase subunit Arg340His	G11778A	Anti-sense	Wild	**ACGGACGCGGAG**gcatcataatcctctctcaag	63.5	RED
			Mutant	**CGCGCCGAGG**acatcataatcctctctcaag	62.2	FAM
			Invader	gcctagcaaactcaaactacgaacgcactcacagtct	77.7	
NADH dehydrogenase subunit Met64Val	T14484C	Sense	Wild	**CGCGCCGAGG**atggttgtctttggatatactac	63.4	FAM
			Mutant	**ACGGACGCGGAG**gtggttgtctttggatatacta	62.8	RED
			Invader	ttttgggggaggttatatgggtttaatagttttttaatttatttaggggaatgt	76.0	

The Large letters indicates the flap sequences of primary probes.

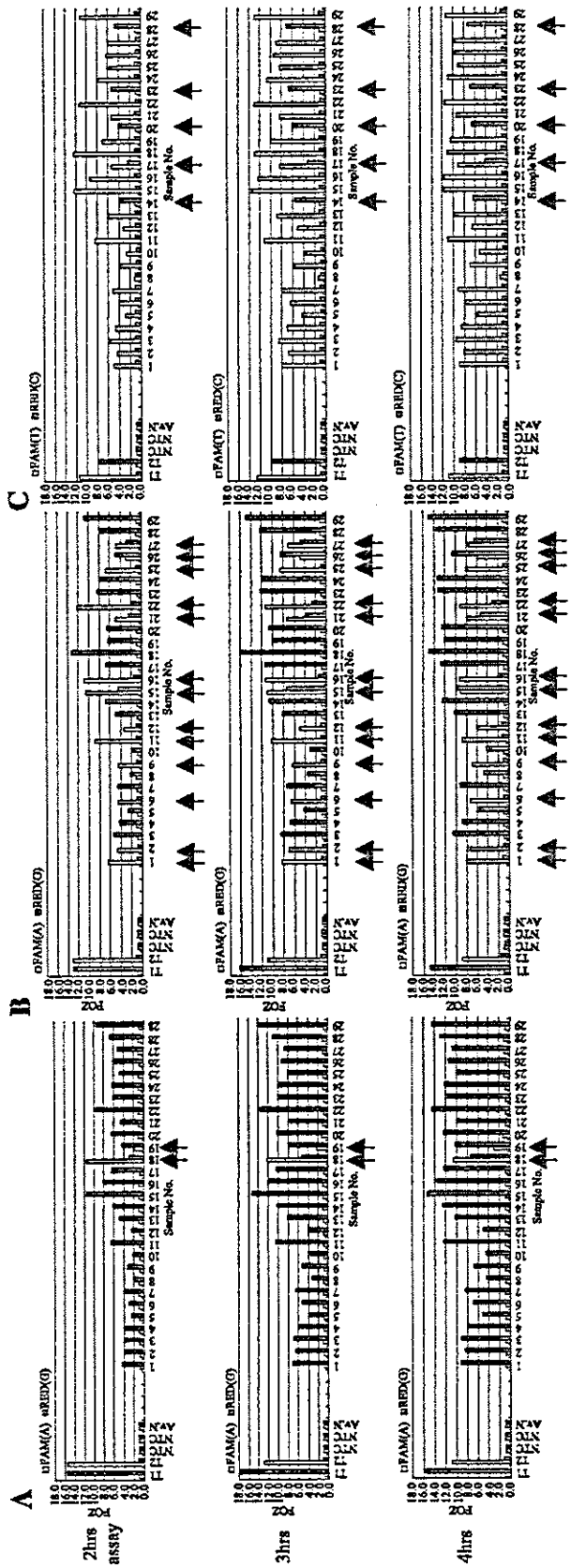

Fig. 3. Detection of three mutations in mtDNA by Invader® assay for three assay times in 29 patients with bilateral optic neuropathy. (A) G3460A mutation (arrows), (B) G11778A mutation (arrows), and (C) T14484C mutation (arrows).

demonstrate the presence of heteroplasmy or homoplasmy of the three mtDNA mutations.

As the mitochondria contain 2–10 copies of small, double-stranded circular DNA molecules, each cell contains several thousand mtDNA molecules. To determine optimum conditions for the Invader® assay in quantifying the mtDNA heteroplasmy, we prepared 1, 2, 4, 8, 16, 32, 64, and 128 ng of DNA including both genomic and mitochondrial DNAs. The samples were incubated for 1, 2, 3, and 4 h with the primary probe and Invader® oligonucleotide to detect G3460, G11778, or T14484. We constructed an assay time vs. NET FOZ curve in eight different amounts of DNA.

Heteroplasmy quantification by Invader® assay

To determine the level of heteroplasmy by Invader® assay, a standard curve was constructed using 1 pM of synthesized 63-mer oligonucleotides (wild type of G11778: agtccttgagagaggattatgatgcgactgtgagtgcgttcgtagtttgagtttgctaggcag; mutant type of A11778: agtccttgagagaggattatgatgtgactgtgagtgcgttcgtagtttgagtttgctaggcag). Two synthesized oligonucleotides were mixed in appropriate ratios to yield 1 pM in total. The percentage of mutant molecules was calculated by using 100 × allelic ratio/(1 + allelic ratio) or 100 × NET FAM FOZ/(NET FAM FOZ + NET RED FOZ). As the fluorescence intensities of FAM or RED are not the same even in the same molecule, we used the normalized FOZ values described in the Results section.

Results

Detection of mtDNA by Invader® assay

The assay time vs. NET FOZ curves (Assay time–NET FOZ curve) for eight different DNAs (1–128 ng) to detect np G11778 of mtDNA are shown in Fig. 2. For 1–8 ng of DNA, the NET FOZ values increased near linearly with increasing incubation time. However, for 16 and 32 ng of DNA, the assay time–NET FOZ curves were saturated at 3 h after initiating the Invader® assay, and with 64 and 128 ng of DNA, the curves were saturated at 2 h after initiating the assay. From the results, we selected 10 ng of DNA in a 2–3-h assay for detecting mtDNA mutations and quantifying the heteroplasmy by Invader® assay. Under these conditions, the NET FOZ values increased near linearly with the assay time. The same results were obtained for np G3460 and T14484 of mtDNA by Invader® assay (data not shown).

Under these conditions, 100 normal controls showed almost zero NET RED FOZ value (mutant probe) for G3460A and G11778A mutations, and zero NET FAM FOZ value (mutant probe) for T14484C mutation (data not shown).

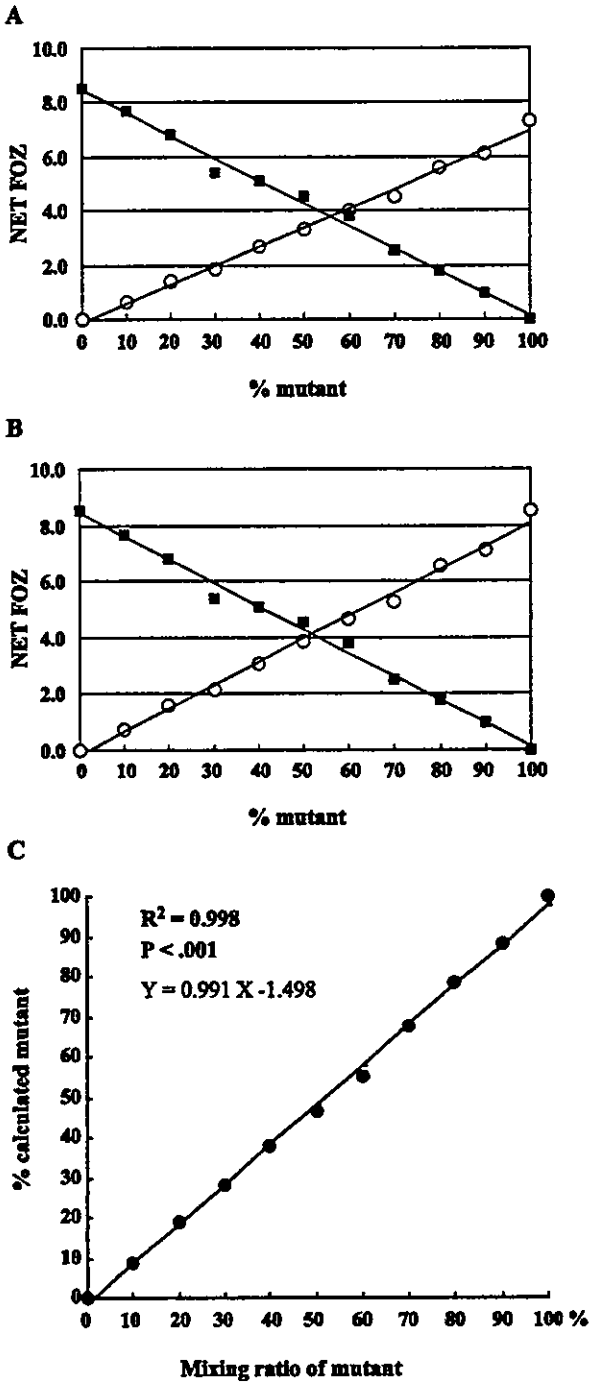

Fig. 4. Quantification of heteroplasmy of the G11778A mutant by Invader® assay. (A) NET FAM FOZ (mutant A11778: open circles) or NET RED FOZ (wild-type G11778: closed squares) vs. % mutant curves in a 2-h assay. (B) Modified NET FAM FOZ (mutant A11778: open circles) or NET RED FOZ (wild-type G11778: closed squares) vs. % mutant curves in a 2-h assay. (C) Standard plots for mutant oligonucleotides with G11778A quantified by the Invader® assay.